2

Spectral Profile Modifications In Metal-Enhanced Fluorescence

E. C. Le Ru[a]*, J. Grand[b], N. Félidj[b], J. Aubard[b], G. Lévi[b], A. Hohenau[c], J. R. Krenn[c], E. Blackie[a], P. G. Etchegoin[a]

[a]The MacDiarmid Institute for Advanced Materials and Nanotechnology, School of Chemical and Physical Sciences, Victoria University of Wellington, PO Box 600, Wellington, New Zealand

[b]Laboratoire ITODYS, Université Paris 7 – Denis Diderot, CNRS UMR 7086, 1 rue Guy de la Brosse, F - 75005 Paris, France

[c]Institute of Physics, Karl Franzens University, Universit¨atsplatz 5, A-8010 Graz, Austria

2.1 INTRODUCTION

In this chapter, we provide a tutorial review of an often-overlooked aspect of Metal Enhanced Fluorescence (MEF), namely the modification of the spectral profile of emission [1]. Decay rates (radiative and total) of a fluorophore are strongly modified in MEF conditions, as a result of electromagnetic (EM) coupling to localized surface plasmon (LSP) resonances in the metallic substrate [2,3,4,5,6,7,8,9,10,11,12]. These decay rate modifications are, as the underlying LSP resonances, wavelength-dependent, a fact that has recently been discussed in detail [13]. These well-accepted facts should naturally result in a modification of the spectral profile of fluorescence in MEF conditions, in addition to the "standard" modifications of the fluorescence intensity (enhancement or quenching). Despite this, spectral profile modifications (SPMs) in MEF conditions have hardly been discussed in the literature, neither theoretically nor experimentally. Up until recently, there had only been isolated reports of small SPMs, typically mentioned in passing in studies dedicated to other aspects of MEF [11, 14]. We have presented in Ref. [1] a theoretical and experimental study dedicated entirely to this particular aspect of MEF (called Surface Enhanced Fluorescence (SEF) in Ref. [1]; MEF and SEF will be used with the same meaning in this chapter). The content of this chapter is therefore largely based on an extension of the concepts and results of Ref. [1], where several of the mechanisms of Spectral Profile Modification (SPM) discussed below were first proposed and evidenced.

This chapter is organized as follows. In Sec. 2.2, we review some basic aspects of the free-space fluorescence process and of its modification close to metal surfaces (MEF). These concepts are then extended in Sec. 2.3 to discuss the various mechanisms of spectral profile modification that can be expected in MEF conditions. Experimental demonstration of some of these concepts is

Spectral Profile Modifications in MEF
Edited by Chris D. Geddes.

provided in Sec. 2.4. Finally, we discuss in Sec. 2.5 some extensions of these concepts and experiments along with possible future research directions.

2.2 PRELIMINARIES

2.2. 1. *Notations And Assumptions*

Let us briefly go through some of the notations and assumptions that will be used throughout this chapter. Units are indicated in brackets [...] when deemed useful.

The fluorophore (emitter) will always be assumed to be embedded in a non-absorbing dielectric medium of refractive index n_M (or relative dielectric constant $\varepsilon_M = (n_M)^2$ real). The excitation is assumed to be monochromatic (e.g. a laser) at angular frequency ω_L [rad s^{-1}]. The excitation density is denoted S_{Inc} [W m^{-2}] (S refers to the Poynting vector). Alternatively, the number of photons per unit area per unit time $N_L = S_{\text{Inc}} / (\hbar\omega_L)$ [m^{-2} s^{-1}] may be used.

The signal (e.g. fluorescence) intensities will be characterized by their powers P [W]. The spectral profile is characterized by the spectral density $n(\omega)$ [rad^{-1}]. By definition, the number of photons per unit time at a frequency between ω and $\omega + d\omega$ is $n(\omega)d\omega$.

The total power is then given by:

$$P = \int \hbar\omega n(\omega) d\omega. \qquad (1)$$

Experimental spectra will be denoted $I(\omega)$ [counts per second, or arb. units] and correspond to the number of photons per unit time, i.e. they are proportional to the spectral density $n(\omega)$.

To avoid unnecessary complications in the presentation, we will ignore any vectorial, tensorial, or molecule orientation effects, unless specifically stated. This does not affect any of the conclusions, and they can always be included at a later stage if judged necessary.

2.2. 2. *Spectral Profile Of Fluorescence: Free-space Case*

In order to discuss any modification to the fluorescence spectral profile, it is important to first understand its origin for a free fluorophore. The model of fluorescence that we discuss below has been simplified as much as possible and retains only the features that are necessary for the generalization to the MEF

case. In particular, most of the parameters of this model are introduced *phenomenologically*. The connection to the underlying molecular electronic and vibrational properties is only discussed qualitatively. More detailed descriptions of the fluorescence process can be found in molecular spectroscopy textbooks [15, 16]. Note that the superscript "0" will be used for all free-space properties, to distinguish them from their modified counterparts in MEF conditions (without superscript).

2.2. 2.a *The Fluorescence Process*

Let us consider a typical fluorophore, with ground (S_0) and excited (S_1) singlet electronic states. The energy states in the vibrational (or vibronic) substructure will be denoted $S_0(\omega_v)$ $S_1(\omega_v)$, where ω_v is the vibrational frequency. The lowest energy state in S_0 (S_1) is accordingly denoted $S_0(0)$ $S_1(0)$. This vibrational substructure is quasi-continuous for most fluorophores (with say, more than ≈ 50 atoms) and can be characterized by a vibrational (or vibronic) density of state $\rho_0(\omega_v)$ in S_0 and $\rho_0(\omega_v)$ in S_1.

The transition energy between $S_0(0)$ and $S_1(0)$ is denoted $\hbar\omega_0$. This fluorophore is excited by monochromatic light (a laser) at angular frequency $\omega_L > \omega_0$. The fluorescence process is represented schematically in the simplified Jablonski diagram of Fig. 2.1(a) (see Sec. 2.3) and consists of three separate steps.

Absorption:

The first step corresponds to the absorption of a photon (of energy $\hbar\omega_L$), resulting in the excitation of an electron from the ground (S_0) to the excited electronic state (S_1). More precisely, the transition occurs from a state $S_0(\omega_{v0})$in the substructure of S_0 to a state $S_1(\omega_{v1})$ in the substructure of S_1 and energy conservation therefore requires $\omega_{v1} - \omega_{v0} + \omega_0 = \omega_L$. Moreover, at thermal equilibrium at a temperature T, the probability of occupation for the initial electron in S_0 can in principle be determined from $\rho_0(\omega_v)$ (and is typically within a range $\sim k_B T$ from $S_0(0)$). At room temperature the energy $k_B T$ is of the order of 200 cm^{-1} and we will assume for simplicity that it is negligible compared to the other energy scales in the system. This is equivalent to assuming $T = 0$ K and neglecting any thermal excitation effects. In this case the initial state for the transition is $S_0(0)$.

Optical absorption can be described in terms of the absorption cross section σ^0_{Abs} [m^2] of the molecule. For excitation at ω_L, the power absorbed is then given by:

$$P^0_{\text{Abs}} = \sigma^0_{\text{Abs}}(\omega_L) S_{\text{Inc}} \qquad (2)$$

For fluorophores, $\sigma^0_{\text{Abs}}(\omega_L)$ can easily be measured experimentally in UV / V is absorption experiments. Note that the spectral profile of absorption is intricately related to the vibrational density of state $\rho_1(\omega_v)$ (and more precisely to overlap integrals between vibrational states within the Franck-Condon approximation). It can therefore be used as an experimental probe of the vibrational density of state.

Relaxation:

The second step is then that of energy relaxation within the excited state S_1. This typically occurs through vibrational relaxation (or possibly through interactions with the environment) on picosecond time-scales; sometimes even hundreds of femtoseconds for large molecules. This step is probably the least understood, but is in most cases irrelevant because it is much faster than the other processes. It results, in fact, in fast thermalization of the excited electron in S_1. Neglecting thermal excitation, the electron reaches the lowest state $S_1(0)$, typically within picoseconds [15].

Decay:

The final step corresponds to the decay of the electron from $S_1(0)$ to a state $S_0(\omega_v)$ in the substructure of the electronic ground state. This decay may be radiative, i.e. it results in emission of a photon at angular frequency $\omega_S = \omega_0 - \omega_v$; this is what is detected as fluorescence. It may also be non-radiative and the energy is then lost to other degrees of freedom in the system (for example to internal rotations, to the solvent, or to the triplet state). All decay mechanisms are stochastic processes and are therefore characterized by their probability of occurring per unit time or rate; in this case the radiative decay rate Γ^0_{Rad} and the non-radiative decay rate Γ^0_{NR}. The total decay rate is then $\Gamma^0_{\text{Tot}} = \Gamma^0_{\text{Rad}} + \Gamma^0_{\text{NR}}$ and $(\Gamma^0_{\text{Tot}})^{-1}$ is the excited state lifetime. Moreover all possible decay paths compete with each other. The quantum yield Q^0 – corresponding to the proportion of electrons decaying radiatively– is then defined as $Q^0 = \Gamma^0_{\text{Rad}} / \Gamma^0_{\text{Tot}}$. Following decay to S_0, the absorption / relaxation / emission cycle can then start again.

In this simple description, we have not considered possible additional effects such as: excitation to a higher excited state, saturation effects, or inter-system crossing (transition to the triplet state). These will be ignored throughout for simplicity.

In most fluorescence models where the spectral profile is ignored, the emitted fluorescence power is then simply given as $P^0_{\text{Fluo}} = \sigma^0_{\text{Abs}} Q^0 S_{\text{Inc}}$. This can alternatively be characterized by a fluorescence cross-section: $\sigma^0_{\text{Fluo}} = \sigma^0_{\text{Abs}} Q^0$. We now adapt this standard argument to account for the spectral dispersion.

2.2. 2.b *A Model For The Spectral Profile*

The spectral profile of fluorescence is characterized by the ω_S-dependence of the fluorescence intensity. Within the simple description given above, it is therefore governed by the final step in the process, i.e. decay from $S_1(0)$ to $S_0(\omega_v)$, which we now study in more detail.

We first need to define the radiative decay rate at frequency ω_S. Because of the continuous nature of ω_S, we have to consider all transitions from $S_1(0)$ to $S_0(\omega_v = \omega_0 - \omega)$ at frequencies ω within a small frequency range: $\omega_S \le \omega \le \omega_S + d\omega_S$. Their radiative decay rate is by definition $\gamma^0_{\text{Rad}}(\omega_S) d\omega_S$. $\gamma^0_{\text{Rad}}(\omega_S)$ [rad^{-1}] can be viewed as the spectral density of the radiative decay rate. This will in most cases be a parameter determined by experiments, but is in principle directly related to the ground state vibrational density of state $\rho_0(\omega_v)$ (and to overlap integrals within the Franck-Condon approximation). The (total) radiative decay rate is then obtained by integration of its spectral density over the entire fluorescence spectrum, i.e.

$$\Gamma^0_{\text{Rad}} = \int \gamma^0_{\text{Rad}}(\omega_S) d\omega_S . \qquad (3)$$

The non-radiative decay rate is Γ^0_{NR} as before (its spectral density is irrelevant here) and the total decay rate is therefore as before $\Gamma^0_{\text{Tot}} = \Gamma^0_{\text{Rad}} + \Gamma^0_{\text{NR}}$. The spectral density of the radiated (fluorescence) signal is then:

$$n^0_{\text{Rad}}(\omega_S) = \frac{\gamma^0_{\text{Rad}}(\omega_S)}{\Gamma^0_{\text{Tot}}} \sigma^0_{\text{Abs}} N_L . \qquad (4)$$

The spectral profile of fluorescence is therefore entirely determined (phenomenologically) by the ω_S-dependence of $\gamma^0_{\text{Rad}}(\omega_S)$. This is linked, microscopically, to the density of states $\rho_0(\omega_0 - \omega_S)$ in the substructure of S_0 and the matrix elements of the respective transitions (or overlap integrals of the vibrational states).

The total fluorescence power is then obtained using Eqs. 1 and 4 as

$$P_{\text{Fluo}}^{0} = Q^{0-\text{Eff}} \sigma_{\text{Abs}}^{0} S_{\text{Inc}} \quad \text{with} \quad Q^{0-\text{Eff}} = \frac{\Gamma_{\text{Rad}}^{0-\text{Eff}}}{\Gamma_{\text{Tot}}^{0}}, \tag{5}$$

where $Q^{0-\text{Eff}}$ is an effective quantum yield and the effective radiative decay rate has been defined as:

$$\Gamma_{\text{Rad}}^{0-\text{Eff}} = \int \frac{\omega_S}{\omega_L} \gamma_{\text{Rad}}^{0}(\omega_S) d\omega_S . \tag{6}$$

It is interesting to highlight the fact that, strictly speaking, the effective radiative decay $\Gamma_{\text{Rad}}^{0-\text{Eff}}$ that enters this expression is different to the real radiative decay rate Γ_{Rad}^{0} that may be measured in a time-resolved experiment (if Γ_{NR}^{0} is known). However, in most practical cases, it is easy to see that $\Gamma_{\text{Rad}}^{0-\text{Eff}} \approx \Gamma_{\text{Rad}}^{0}$ to a very good approximation (since $\omega_L - \omega_S \ll \omega_S$). We will therefore ignore this distinction in the following.

We have here kept the description of the radiative decay rates fairly general and did not discuss their exact relations to the vibronic states (in particular within the Franck-Condon approximation). This description is sufficient for our purpose here and more adapted to the generalization to the case of MEF. It is nevertheless worth mentioning that there is an approximate symmetry between the transitions for absorption: $S_0(0) \rightarrow S_1(\omega_v)$ and those for fluorescence emission: $S_1(0) \rightarrow S_0(\omega_v)$. This results in the well-known "mirror symmetry" around the $\omega = \omega_0$ line between the absorption and fluorescence spectra, i.e. $P_{\text{Fluo}}^{0}(\omega) \propto P_{\text{Abs}}^{0}(2\omega_0 - \omega)$.

2.2. 3. *Plasmonic Effects In MEF Conditions*

We are now looking at extending the simple model for free-space fluorescence to the case of Metal Enhanced Fluorescence (MEF). We therefore consider a fluorophore with known free-space properties in the presence of optically-active objects (in particular metallic objects).

The EM theory of Metal Enhanced Fluorescence (MEF) was studied and developed extensively in the 70-80's [2,3,4,5,6]. All the EM mechanims involved in MEF can be understood within classical EM theory [3,4,5,6] as confirmed in the simplest cases by quantum studies [2,12,17,18]. In most of these models, the emitter is depicted as a simple two- (or three-) level system, i.e. only one emission wavelength is considered. This is appropriate in general to understand modifications of absorption or emission rates, but it entirely ignores the spectral profile of the fluorescence emission. We will first review

these concepts here before extending and generalizing them in the next section (to specifically incorporate the description of the fluorescence spectral profile in MEF conditions).

When a fluorophore is located in close proximity to a metal surface, both its absorption and emission properties may be affected dramatically. This in turn affects its fluorescence properties and may result in either a quenching or an enhancement of the fluorescence signal. This latter situation is obviously of interest for many applications using fluorophores. Let us discuss these steps in more detail.

2.2. 3.a *The Local Field Enhancement*

We focus first on the absorption. It is well known that the electric field may change dramatically in the vicinity of metallic surfaces, both in magnitude and polarization. The modified field at the molecule position, which we call the local field $\mathbf{E}_{\mathrm{Loc}}(\omega_L)$, can in principle be deduced and calculated at every point by solving the EM problem with appropriate boundary conditions. The field intensity felt by the molecule is modified by the local field intensity enhancement factor (EF):

$$M_{\mathrm{Loc}}(\omega_L) = \frac{|\mathbf{E}_{\mathrm{Loc}}(\omega_L)|^2}{|E_{\mathrm{Inc}}|^2}, \tag{7}$$

where E_{Inc} is the electric field amplitude of the incident excitation. One can then show that the absorption cross-section (or power absorbed) is modified by the same factor, i.e.:

$$\sigma_{\mathrm{Abs}}(\omega_L) = M_{\mathrm{Loc}}(\omega_L)\sigma^0_{\mathrm{Abs}}(\omega_L). \tag{8}$$

2.2. 3.b *Radiative And Non-Radiative Enhancements*

Similar modifications arise for the emission properties of an emitter and affect its radiative decay. We will assume that the intrinsic non-radiative decay path is unchanged (a reasonable assumption since it does not involve photons) and is therefore characterized by the same rate Γ^0_{NR}. The radiative decay path, characterized by Γ^0_{Rad} in free-space, is modified in at least three ways:

- Firstly, the decay rate through photon emission is modified and we will call the modified rate the total EM decay rate $\Gamma^{\mathrm{EM}}_{\mathrm{Tot}}$. The EM superscript indicates the EM nature of the decay (through emission of a photon).

- Secondly, part of the photons emitted during this decay may be absorbed in the environment (for example the metal substrate). These photons are not radiated in the far-field; they correspond to non-radiative

emission. Such a non-radiative decay is very different in nature to the intrinsic non-radiative channel, since it does involve exchange of a photon. From an experimental point of view, however, the end result is the same, i.e. a decay without production of a fluorescence photon. To distinguish the two possible EM decay channels, we can define the radiative Γ_{Rad} and non-radiative Γ_{NR}^{EM} EM decay rates, the sum of which gives Γ_{Tot}^{EM}. One can alternatively define the EM radiative efficiency $\eta_{Rad}^{EM} = \Gamma_{Rad} / \Gamma_{Tot}^{EM}$. All these decay rates can instead be characterized with respect to the free-space EM decay rate (i.e. the free-space radiative decay rate) by defining the total EM enhancement factor, the non-radiative EM enhancement factor, and the radiative enhancement factor as:

$$M_{Tot} = \frac{\Gamma_{Tot}^{EM}}{\Gamma_{Rad}^{0}} \quad M_{NR} = \frac{\Gamma_{NR}^{EM}}{\Gamma_{Rad}^{0}} \quad M_{Rad} = \frac{\Gamma_{Rad}}{\Gamma_{Rad}^{0}}. \tag{9}$$

The EM radiative efficiency is then given as

$$\eta_{Rad}^{EM} = \frac{M_{Rad}}{M_{Tot}}. \tag{10}$$

❖ Thirdly, the radiation pattern (angular and polarization dependence of the radiated power) may also be modified. We will ignore this aspect, which is in most cases secondary.

The total decay rate of the emitter is the sum of the decay rates for all possible decay channels (which compete with each other) and is therefore:

$$\Gamma_{Tot} = \Gamma_{Tot}^{EM} + \Gamma_{NR}^{0} = M_{Tot}\Gamma_{Rad}^{0} + \Gamma_{NR}^{0}. \tag{11}$$

This is what would be observable in time-resolved experiments; the lifetime being simply $(\Gamma_{Tot})^{-1}$ [7].

2.2. 3.c *Fluorescence Enhancement Factor*

The modified quantum yield can therefore be expressed as:

$$Q = \frac{\Gamma_{Rad}}{\Gamma_{Tot}} = \frac{M_{Rad}}{M_{Tot} + \Gamma_{NR}^{0} / \Gamma_{Rad}^{0}} = \frac{M_{Rad}}{M_{Tot} + (Q^{0})^{-1} - 1} \approx \eta_{Rad}^{EM}, \tag{12}$$

where the latter approximation is valid when $M_{Tot} \gg (Q^{0})^{-1}$, which is the case in most situations of interests. Note that this means that the modified quantum yield is determined entirely by the EM radiative efficiency, a property

of the metallic substrate. All fluorophores should therefore have the same modified quantum yield, irrespective of their intrinsic quantum yield Q^0 (see for example Ref. [19] for a discussion of the EM factors affecting the modified quantum yield, along with examples of MEF predictions on spherical metallic nanoparticles).

The modified fluorescence power can be expressed, as in the free space case, as $P_{\text{Fluo}} = Q\sigma_{\text{Abs}}S_{\text{Inc}}$. This may conveniently be expressed as a fluorescence enhancement factor:

$$M_{\text{Fluo}} = \frac{P_{\text{Fluo}}}{P^0_{\text{Fluo}}} = M_{\text{Loc}} \frac{M_{\text{Rad}}}{Q^0 M_{\text{Tot}} + 1 - Q^0} \approx M_{\text{Loc}} \frac{M_{\text{Rad}}}{Q^0 M_{\text{Tot}}} = \frac{M_{\text{Loc}} \eta^{\text{EM}}_{\text{Rad}}}{Q^0}. \quad (13)$$

The fluorescence enhancement is therefore a result of the interplay of three factors:

- The local field enhancement factor M_{Loc}, characterizing the modification of absorption. This results, in most cases of interest, in an enhancement, and possibly a very large enhancement up to $\approx 10^5$.

- The EM radiative efficiency $\eta^{\text{EM}}_{\text{Rad}} = M_{\text{Rad}} / M_{\text{Tot}}$. This is always smaller (and possibly much smaller) than 1, and contributes to a quenching of the fluorescence because of non-radiative emission (fluorescence photons absorbed in the metallic substrate).

- The factor $(Q^0)^{-1}$, an intrinsic property of the fluorophore under consideration. For a good fluorophore with $Q^0 \approx 1$, this factor has no effect. Only for a bad fluorophore with $Q^0 \ll 1$ can this factor lead to a substantial additional fluorescence enhancement. This is, in a way, a consequence of the fact that the modified quantum yield is dictated by the metallic substrate and therefore the same for all fluorophores (good or bad). If one uses a bad fluorophore, greater enhancements can be obtained simply because the free-space fluorescence was poor in the first place.

The exact balance among these three factors determines whether fluorescence quenching or enhancement is observed [10].

2.2. 3.d *Link Between The Local Field And Radiative Enhancement Factors*

The local field and decay rate enhancements have the same physical origin: EM coupling to the plasmon resonances of the metallic substrate. This will be discussed in more detail in Sec. 3.7. All these enhancement factors

therefore exhibit a strong wavelength- (or equivalently ω-) dependence. This fact will actually be the main reason for the spectral profile medifications predicted in the MEF signal.

Moreover, it is possible to show that the local field enhancement factor $M_{\mathrm{Loc}}(\omega)$ and the radiative enhancement factor $M_{\mathrm{Rad}}(\omega)$ are in many cases of the same order of magnitude. The exact relation between these and the range of validity of the statement above are not trivial and require the use of the optical reciprocity theorem; see for example Refs. [20, 21] for more details. The approximation $M_{\mathrm{Loc}}(\omega) \approx M_{\mathrm{Rad}}(\omega)$ is nevertheless very useful when discussing (semi-quantitatively) the magnitude of the fluorescence enhancement or quenching.

2.3 SPECTRAL PROFILE IN MEF CONDITIONS

Due to the intrinsic spectral dependence of localized surgace Plasmon resonances, all the enhancement factors defined so far for emission depend on ω_S (the emission frequency). This should, accordingly, affect the spectral profile of MEF

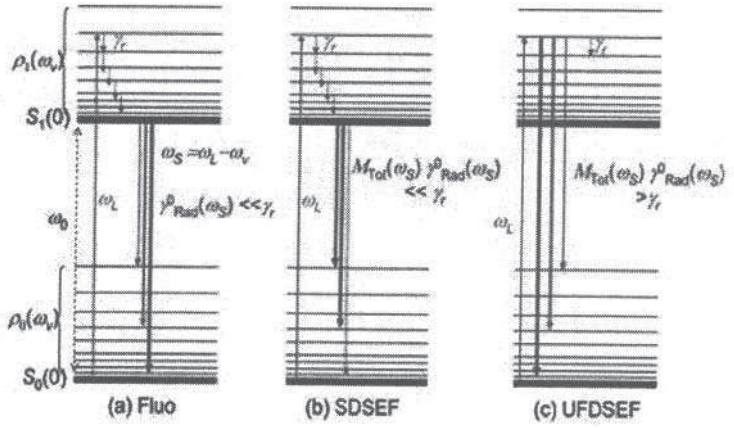

Figure 2.1: Adapted and reproduced with permission from *J. Phys. Chem. C* 2007, *111*, 16076–16079. Copyright 2007 American Chemical Society. Simplified Jablonski diagrams depicting the processes involved for a fluorophore in three possible situations discussed in the text: (a) Standard fluorescence, (b) Surface Enhanced Fluorescence in the slow-dynamics regime (SDMEF), and (c) MEF in the ultra-fast-dynamics regime (UFDMEF).

2.3. 1. *The Regimes Of Spectral Profile Modification*

We have assumed so far that the electron has sufficient time to relax within the substructure of S_1 and therefore reach the lowest state $S_1(0)$ before any decay to the ground state occurs. This is entirely justified if the total decay rate from S_1 is much smaller than the typical internal relaxation rate in S_1, γ_r. In MEF conditions however, the factor M_{Tot} (and therefore the total decay rate Γ_{Tot}) may be large enough for this common assumption to become no longer justified. This possibility has in fact been occasionally suggested in the past [22, 23], but never actually pursued. If this is the case, the dynamics of the electron in the substructure of S_1 then becomes important. It is therefore necessary to distinguish between three regimes for MEF.

Following the notations of Ref. [1], these are:

- Slow-dynamics MEF (SDMEF), for which $\Gamma_{\text{Tot}} \ll \gamma_r$. This is the same situation as for standard MEF. The electron relaxes to $S_1(0)$ from which it can then decay to S_0.

- Fast-dynamics MEF (FDMEF), for which Γ_{Tot} is of the order of –and possibly larger than– the internal relaxation rate γ_r. In this case, decay to the ground state may occur from any intermediate levels $S_1(\omega_v)$ between the one reached after absorption $S_1(\omega_L - \omega_0)$ and the lowest one $S_1(0)$.

- Ultra-fast-dynamics MEF (UFDMEF), for which $\Gamma_{\text{Tot}} \gg \gamma_r$. In this extreme case of FDMEF, the decay rate is so fast that no energy relaxation occurs in S_1. All decay transitions therefore occur from $S_1(\omega_L - \omega_0)$.

Note that the distinction between SDMEF and FDMEF is irrelevant in cases where the excitation energy ω_L is close to or below the transition energy ω_0. The fluorescence process in the SDMEF and UFDMEF regimes are represented schematically in simplified Jablonski diagrams in Fig. 2.1 along with the standard fluorescence process for comparison. We will now extend the models described so far to these three regimes of spectral profile modification of the MEF.

2.3. 2. *Slow-Dynamics Regime*

In the slow-dynamics regime (see Fig. 2.1(b)), the situation is very similar to standard fluorescence (Fig. 2.1(a)), except for the rate modifications introduced by the metallic substrate.

2.3. 2.a *Modified Decay Rates*

Let us consider again the transitions between $S_1(0)$ to $S_0(\omega_0 - \omega_S)$ at an energy $\hbar\omega_S$. The modified spectral density of the radiative decay rate is

$$\gamma_{\mathrm{Rad}}(\omega_S) = M_{\mathrm{Rad}}(\omega_S)\gamma^0_{\mathrm{Rad}}(\omega_S), \tag{14}$$

and there is a corresponding spectral density for non-radiative EM emission:

$$\gamma_{\mathrm{NR}}(\omega_S) = M_{\mathrm{NR}}(\omega_S)\gamma^0_{\mathrm{Rad}}(\omega_S). \tag{15}$$

The total EM decay rate is accordingly:

$$\Gamma^{\mathrm{EM}}_{\mathrm{Tot}} = \int (\gamma_{\mathrm{Rad}}(\omega_S) + \gamma_{\mathrm{NR}}(\omega_S))d\omega_S = \int M_{\mathrm{Tot}}(\omega_S)\gamma^0_{\mathrm{Rad}}(\omega_S)d\omega_S. \tag{16}$$

It is convenient here to define the *spectrally averaged total EM enhancement factor* as:

$$\bar{M}_{\mathrm{Tot}} = \int M_{\mathrm{Tot}}(\omega_S)\frac{\gamma^0_{\mathrm{Rad}}(\omega_S)}{\Gamma^0_{\mathrm{Rad}}}d\omega_S. \tag{17}$$

In a similar fashion, the *spectrally averaged radiative decay rate enhancement factor* is:

$$\bar{M}_{\mathrm{Rad}} = \int M_{\mathrm{Rad}}(\omega_S)\frac{\gamma^0_{\mathrm{Rad}}(\omega_S)}{\Gamma^0_{\mathrm{Rad}}}d\omega_S. \tag{18}$$

Note that the weighing factor $\gamma^0_{\mathrm{Rad}}(\omega_S)$ in these integrals is proportional to the free-space fluorescence spectral density $n^0_{\mathrm{Rad}}(\omega_S)$, which can be measured easily experimentally.

Thus, we have simply:

$$\Gamma^{\mathrm{EM}}_{\mathrm{Tot}} = \bar{M}_{\mathrm{Tot}}\Gamma^0_{\mathrm{Rad}}, \text{ and } \quad \Gamma_{\mathrm{Rad}} = \bar{M}_{\mathrm{Rad}}\Gamma^0_{\mathrm{Rad}}. \tag{19}$$

$\bar{M}_{\mathrm{Tot}}$ and $\bar{M}_{\mathrm{Rad}}$ then play the same role that $M_{\mathrm{Tot}}(\omega_S)$ and $M_{\mathrm{Rad}}(\omega_S)$ did in the one-wavelength fluorescence model. The modified total decay rate is then

$$\Gamma_{\mathrm{Tot}} = \Gamma_{\mathrm{Tot}}^{\mathrm{EM}} + \Gamma_{\mathrm{NR}}^{0} = \left(\bar{M}_{\mathrm{Tot}} + (Q^0)^{-1} - 1\right)\Gamma_{\mathrm{Rad}}^{0}. \qquad (20)$$

2.3. 2.b *Modified Spectral Profile*

The modified spectral density is obtained (as for the free-space case) from:

$$n_{\mathrm{Rad}}^{\mathrm{SDSEF}}(\omega_S) = \frac{\gamma_{\mathrm{Rad}}(\omega_S)}{\Gamma_{\mathrm{Tot}}}\sigma_{\mathrm{Abs}}N_L = \frac{M_{\mathrm{Rad}}(\omega_S)\gamma_{\mathrm{Rad}}^{0}(\omega_S)}{\Gamma_{\mathrm{Tot}}}\sigma_{\mathrm{Abs}}N_L. \qquad (21)$$

From this expression, the MEF spectral profile is simply determined through the product of the free-space spectral profile, proportional to $\gamma_{\mathrm{Rad}}^{0}(\omega_S)$ and the radiative enhancement factor profile $M_{\mathrm{Rad}}(\omega_S)$. This can, in fact, be expressed as a modification factor with respect to the free-space case as:

$$\frac{n_{\mathrm{Rad}}^{\mathrm{SDSEF}}(\omega_S)}{n_{\mathrm{Rad}}^{0}(\omega_S)} = \frac{M_{\mathrm{Rad}}(\omega_S)}{\bar{M}_{\mathrm{Tot}} + (Q^0)^{-1} - 1}M_{\mathrm{Loc}}(\omega_L). \qquad (22)$$

The ω_S-dependence in this modification factor is entirely dictated by $M_{\mathrm{Rad}}(\omega_S)$.

2.3. 2.c *Fluorescence Intensity*

This latest expression provides in addition the magnitude of the fluorescence intensity enhancement factor at a given frequency ω_S. In some instances and also to make a connection with the standard one-wavelength model, it may be more convenient to consider the total fluorescence intensity.

Following the description above, the *modified quantum yield* is simply obtained as:

$$Q = \frac{\Gamma_{\mathrm{Rad}}}{\Gamma_{\mathrm{Tot}}} = \frac{\bar{M}_{\mathrm{Rad}}}{\bar{M}_{\mathrm{Tot}} + (Q^0)^{-1} - 1}. \qquad (23)$$

Similarly, the *total fluorescence power enhancement factor* is:

$$M_{\text{Fluo}} = \frac{P_{\text{Fluo}}}{P^0_{\text{Fluo}}} = \frac{\bar{M}^{\text{Eff}}_{\text{Rad}}}{\bar{M}_{\text{Tot}} + (Q^0)^{-1} - 1} M_{\text{Loc}}(\omega_L), \tag{24}$$

where

$$\bar{M}^{\text{Eff}}_{\text{Rad}} = \int \frac{\omega_S}{\omega_L} M_{\text{Rad}}(\omega_S) \frac{\gamma^0_{\text{Rad}}(\omega_S)}{\Gamma^0_{\text{Rad}}} d\omega_S. \tag{25}$$

In a similar manner to the free-space case, $\bar{M}^{\text{Eff}}_{\text{Rad}}$ (for the power enhancement) is strictly speaking different to $\bar{M}_{\text{Rad}}$ (for the rate enhancement) because of the Stokes shift, but for most practical purposes, $\bar{M}^{\text{Eff}}_{\text{Rad}} \approx \bar{M}_{\text{Rad}}$ is a very good approximation. These expressions for the modified quantum yield and the fluorescence enhancement factor are therefore essentially the same as those obtained in the one-wavelength model, only replacing $M_{\text{Rad}}(\omega_S)$ and $M_{\text{Tot}}(\omega_S)$ by $\bar{M}_{\text{Rad}}$ and $\bar{M}_{\text{Tot}}$. This is an important result, since it means that, as far as the total fluorescence intensity is concerned, any spectral modification can in a first approximation be ignored, and a one-wavelength model (at the frequency of the fluorescence peak ω_F) can be used. Hence, the discussion of the various mechanisms of fluorescence enhancement and quenching given in Sec. 2.2 3 remains valid.

2.3. 3. *Ultra-Fast-Dynamics Regime*

2.3. 3.a *Model*

The ultra-fast-dynamics regime is, in some ways, similar to the slow-dynamics regime; the only difference being that the decay transitions originate from $S_1(\omega_L - \omega_0)$ rather than $S_1(0)$. Let us denote $\Delta\omega_L = \omega_L - \omega_0$ and assume here that $\Delta\omega_L > 0$. If ω_L is close to or smaller than ω_0, then internal relaxation in S_1 is irrelevant and the treatment given for the SDMEF applies independently of the actual decay rates.

In order to adapt the previous description, one therefore only needs to replace the free-space spectral decay rates from $S_1(0)$, $\gamma^0_{\text{Rad}}(\omega_S)$, by those from $S_1(\Delta\omega_L)$, denoted $\gamma^1_{\text{Rad}}(\omega_S)$ in the following. In a first approximation, one may assume that the dipole moment (or overlap integrals) is the same for both transitions. Therefore, what determines their decay rate is primarily the density of states in the final state in S_0 (and the secondary ω^3 dependence of decay rates, which we also neglect here). Accordingly, we can assume that the two transitions to the same final state, $S_1(\Delta\omega_L) \rightarrow S_0(\omega_L - \omega_S)$ (at

frequency ω_S) and $S_1(0) \rightarrow S_0(\omega_L - \omega_S)$ (at frequency $\omega_S - \Delta\omega_L$), have (in a first approximation) the same decay rate, i.e.:

$$\gamma^1_{\mathrm{Rad}}(\omega_S) \approx \gamma^0_{\mathrm{Rad}}(\omega_S - \Delta\omega_L). \tag{26}$$

From there, all the formula of the previous section apply, simply replacing $\gamma^0_{\mathrm{Rad}}(\omega_S)$ by $\gamma^0_{\mathrm{Rad}}(\omega_S - \Delta\omega_L)$.

In particular, we have:

$$\bar{M}^{\mathrm{UFDSEF}}_{\mathrm{Tot}} = \int M_{\mathrm{Tot}}(\omega_S) \frac{\gamma^0_{\mathrm{Rad}}(\omega_S - \Delta\omega_L)}{\Gamma^0_{\mathrm{Rad}}} d\omega_S. \tag{27}$$

Note that $\bar{M}^{\mathrm{UFDSEF}}_{\mathrm{Tot}}$ is of the same order of magnitude as that obtained for SDMEF (Eq. 17). The spectral density of fluorescence in the UFDMEF regime is then:

$$n^{\mathrm{UFDSEF}}_{\mathrm{Rad}}(\omega_S) = \frac{M_{\mathrm{Rad}}(\omega_S)\gamma^0_{\mathrm{Rad}}(\omega_S - \Delta\omega_L)}{\Gamma^{\mathrm{UFDSEF}}_{\mathrm{Tot}}} \sigma_{\mathrm{Abs}} N_L. \tag{28}$$

This expression is similar to that obtained for the SDMEF case (Eq. 21), except that the radiative enhancement factor $M_{\mathrm{Rad}}(\omega_S)$ is now applied to the *blue-shifted free-space fluorescence profile* $\gamma^0_{\mathrm{Rad}}(\omega_S - \Delta\omega_L)$. It can, in fact, be expressed as a modification factor with respect to the blue-shifted free-space case as:

$$\frac{n^{\mathrm{UFDSEF}}_{\mathrm{Rad}}(\omega_S)}{n^0_{\mathrm{Rad}}(\omega_S - \Delta\omega_L)} = \frac{M_{\mathrm{Rad}}(\omega_S)}{\bar{M}^{\mathrm{UFDSEF}}_{\mathrm{Tot}} + (Q^0)^{-1} - 1} M_{\mathrm{Loc}}(\omega_L). \tag{29}$$

It is possible to also write expressions for the modified quantum yield and fluorescence intensity enhancement factor in the UFDMEF regime. These are similar to those obtained for the SDMEF regime.

2.3. 3.b *Comparison With The SDMEF Regime*

From these results, it is clear that the spectral profile in both the SDMEF and UFDMEF regimes is predominantly dictated by the radiative enhancement factor profile $M_{\mathrm{Rad}}(\omega_S)$. Distinguishing between the two regimes is in principle possible by direct comparison of the respective spectral profile of fluorescence.

They are related by the expression:

$$\frac{n_{\mathrm{Rad}}^{\mathrm{UFDSEF}}(\omega_S)}{n_{\mathrm{Rad}}^{\mathrm{SDSEF}}(\omega_S)} = \frac{n_{\mathrm{Rad}}^{0}(\omega_S - \Delta\omega_L)}{n_{\mathrm{Rad}}^{0}(\omega_S)}. \qquad (30)$$

Such a distinction is facilitated if $\Delta\omega_L$ is large, and in any case requires an accurate knowledge of $n_{\mathrm{Rad}}^{0}(\omega)$ (the difficulties associated with this are discussed in Sec. 2.4).

2.3 4. *Intermediate Regime*

The situation in the intermediate regime is substantially more complicated: both decay to the ground state and energy relaxation can occur from any of the intermediate levels in S_1. The exact dynamics therefore not only depends on the modified decay rates, but also on the details of the relaxation dynamics within S_1; a process that is not understood in detail and is not easily measurable. We will, therefore, not attempt here a detailed description of the intermediate FDMEF regime. Nevertheless, one should qualitatively expect results that reside in between the two limiting cases of SDMEF and UFDMEF.

2.3 5. *Discussion*

Let us summarize the predictions of these simple models in terms of the spectral profile (ω_S -dependence) of the fluorescence:

- The free-space fluorescence spectrum follows $n_{\mathrm{Rad}}^{0}(\omega_S)$.
- The modified spectrum in the SDMEF regime follows $M_{\mathrm{Rad}}(\omega_S) n_{\mathrm{Rad}}^{0}(\omega_S)$.
- The modified spectrum in the UFDMEF regime follows $M_{\mathrm{Rad}}(\omega_S) n_{\mathrm{Rad}}^{0}(\omega_S - \Delta\omega_L)$.

Moreover, for the MEF signal to be observable, it is also necessary that the local field enhancement at the laser frequency $M_{\mathrm{Loc}}(\omega_L)$ is sufficiently large. Since M_{Loc} and M_{Rad} follow approximately the same resonant profile, $M_{\mathrm{Rad}}(\omega_L)$ is a good indication of the magnitude of $M_{\mathrm{Loc}}(\omega_L)$.

For many fluorophores, $n_{\mathrm{Rad}}^{0}(\omega_S)$ is simply a "bell-shaped" curve (for example a Lorentzian); possibly slightly asymmetric or with a shoulder. Its full-width at half-maximum (FWHM) is typically of the order of

$\sim 700-1200$ cm^{-1}. As discussed already, $M_{\mathrm{Rad}}(\omega_S)$ exhibits a resonance profile at frequencies corresponding to the localized surface plasmon (LSP) resonances of the metallic substrate. If a single resonance dominates, its FWHM is typically of the same order as that of the fluorescence spectrum, i.e. $700-1200$ cm^{-1}, for typical Ag or Au substrates in the visible. To understand how such a resonance may affect the MEF spectral profile, it is interesting to consider a few model cases. For the sake of argument, we focus on the cases of Methylene Blue (MB) [24] and Rhodamine 6G (Rh6G) [25] excited at 633 nm, for which the free-space (in water) fluorescence profiles have been measured (dashed lines in Fig. 2.2(a,b,d) for MB and (c) for Rh6G). Note that these free-space fluorescence spectra directly reflect the spectral profile of fluorescence $n^0_{\mathrm{Rad}}(\omega_S)$ as given in Eq. 4. These two examples provide model fluorescence spectra for two typical situations: (i) excitation below (but close to) the absorption maximum (here with $\Delta\omega_L = \omega_L - \omega_0 \approx 900$ cm^{-1} for MB). The fluorescence spectrum then exhibits a strong and broad peak at a smaller energy (Stokes shift), and (ii) excitation at longer wavelength in the absorption tail, $\omega_L < \omega_0$ (the case of Rh6G at 633 nm excitation), where the fluorescence spectrum is much weaker and exhibits a monotonous decay with wavelength. Only residual fluorescence is then observed and, since there is no internal relaxation in S_1 even in the free-space case, the SDMEF and FDMEF regimes are equivalent ($\Delta\omega_L = 0$).

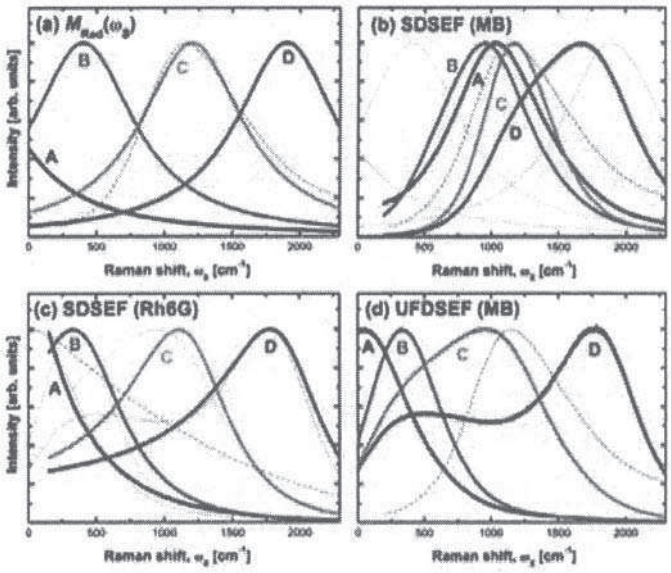

Figure 2.2: Predictions of spectral profile modifications in MEF for a few model cases. Spectra are shown in terms of Raman shift (equivalent to ω_S), assuming a laser excitation at 633 nm. All spectra are normalized to 1. (a) Four model cases of radiation enhancement spectral profile, $M_{\mathrm{Rad}}(\omega_S)$, with a resonance peaking at increasing wavelengths; A: -500 cm^{-1} (614 nm), B: 400 cm^{-1} (650 nm), C: 1200 cm^{-1} (685 nm), and D: 1900 cm^{-1} (720 nm). These are modelled here by Lorenztian profiles with a FWHM of 900 cm^{-1}. The free-space fluorescence spectrum of MB in water ($n^0_{\mathrm{Rad}}(\omega_S)$) is also shown as a dashed line here and in (b) and (d). (b) Predicted SDMEF spectrum of MB, $M_{\mathrm{Rad}}(\omega_S)n^0_{\mathrm{Rad}}(\omega_S)$ for the four cases of (a). The Lorentzian profiles of (a) are repeated as dotted lines for easier comparison. (c) Predicted SDMEF spectrum of Rh6G. Note that this is also the predicted FDMEF spectrum of Rh6G since excitation at 633 nm is below ω_0 (i.e. $\Delta\omega_L = 0$). The free-space spectrum of Rh6G in water [21] is shown as a dashed line (the Raman peaks, observable here because of the weakness of the fluorescence spectrum have been removed). (d) Predicted UFDMEF spectrum of MB, $M_{\mathrm{Rad}}(\omega_S)n^0_{\mathrm{Rad}}(\omega_S - \Delta\omega_L)$ with $\Delta\omega_L = 900$ cm^{-1}. These spectra are repeated as dotted lines in (c) for easier comparison.

The predicted modifications to the MEF spectrum are illustrated in Fig.2. 2 for a few representative radiation enhancement factor profiles $M_{\mathrm{Rad}}(\omega_S)$. These results provide a qualitative overview of what to theoretically expect in terms of Spectral Profile Modification (SPM):

❖ The case of MB in the SDMEF regime (Fig. 2.2(b)) is typical of many MEF experiments. Moreover, to maximize the MEF intensity, the LSP resonance is typically chosen in between the laser excitation and the peak free-space fluorescence emission, i.e. cases B and C in Fig. 2.2(b). Only small SPMs are predicted in these conditions: a small shift for B and a small narrowing for C. These situations are in fact representative of typical MEF conditions and small SPMs should therefore (in general) be expected. Such small modifications have indeed been reported [11], but it is likely that they remain unnoticed or have not been emphasized as such in many cases.

❖ A larger modification is predicted when the resonance occurs beyond the free-space fluorescence peak (case D of Fig. 2.2(b)). The MEF signal is however much smaller because of the small local field enhancement factor at ω_L.

❖ Much more spectacular SPMs are predicted in the case of Rh6G (Fig. 2.2(c)). This can be understood simply: because only the fluorescence tail is excited, the emission is almost flat (featureless) in free-space

and the MEF profile is therefore imposed by the underlying LSP resonance $M_{\mathrm{Rad}}(\omega_S)$ in MEF conditions. Although less common for fluorescence experiments –which will always use excitation close to the absorption maximum of the molecule under use– this situation can be useful, for example, to study the mechanisms of SPMs in MEF and can even be used as a tool to probe the LSP resonances in the substrate.

❖ Another situation where large SPMs are predicted is the case of UFDMEF for MB as shown in Fig. 2.2(d). The predictions are then similar to those of Rh6G (compare solid and dotted lines in 2.2(c)) and this can again be understood simply: in UFDMEF the radiation enhancement factor $M_{\mathrm{Rad}}(\omega_S)$ applies to the blue-shifted free-space fluorescence $n^0_{\mathrm{Rad}}(\omega_S - \Delta\omega_L)$, which typically peaks around ω_L. It therefore applies to the long-wavelength tail of the fluorescence spectrum, which resembles closely that of Rh6G. In fact, this can be generalized to most fluorophores in the UFDMEF regimes: the UFDMEF spectrum is mostly dominated by $M_{\mathrm{Rad}}(\omega_S)$, i.e. by the LSP resonance spectral profile.

2.3 6. *Effect Of Averaging*

In many typical experimental conditions, the fluorescence signal originates from an ensemble of molecules randomly adsorbed on (or close to) the metal substrate. Each of these molecules is therefore subject to different EM enhancement factors, M_{Loc}, M_{Rad}, M_{Tot}, etc...The measured signal should simply be the average signal produced by these individual molecules. Nevertheless, these factors are typically highly non-uniform (spatially) and may exhibit large variations in magnitude, even over relatively small distances [26]. For such distributions, the effect of averaging on complex expressions like Eq. 21 or 24 can be fairly complicated and is beyond the scope of this chapter. This makes predictions of the average absolute fluorescence enhancement a difficult undertaking in general. Fortunately, as far as the spectral profile is concerned, all molecules in the ensemble are subjected to EM enhancement factors originating from the same underlying LSP resonance of the substrate. The modified spectral profile of fluorescence is therefore retained upon spatial averaging, only its absolute magnitude may be affected in a non-trivial way. Nevertheless, there remains the possibility that depending on the spatial distribution of $\bar{M}_{\mathrm{Tot}}$ (and therefore Γ_{Tot}), part of the molecules may be in a different MEF regime than others.

2.3 7. *Fluorescence Intensities In SDMEF And FDMEF Regimes*

2.3 7.a *Qualitative Discussion*

Before moving on to the experimental results, it is worth discussing briefly the conditions (if any) for which FDMEF (or UFDMEF) may be

observed. By definition, this requires the decay rate Γ_{Tot} to be sufficiently large (with respect to internal relaxation rates) or equivalently $\bar{M}_{\text{Tot}}$ to be sufficiently large (say, larger than $\sim 10^4$ for the sake of argument). From Eq. 13 –or its equivalent in FDMEF conditions– this may result in a very poor fluorescence enhancement factor. One may then wonder whether the FDMEF spectrum would be at all observable.

Let us consider two model cases to discuss this issue:

❖ *Radiative-Emission-Dominated Substrate*

Let us take for example the case of a metallic nanoparticle coated with a 10 nm dielectric spacer. The non-radiative emission is then typically negligible and $\bar{M}_{\text{Tot}}$ is of the order of $\bar{M}_{\text{Rad}}$. $\bar{M}_{\text{Rad}}$ may exhibit a strong spatial distribution over the NP surface, but remains below, say $\sim 10^2 - 10^3$. All the molecules are then in the SDMEF regime. Moreover, since $\bar{M}_{\text{Tot}} \approx \bar{M}_{\text{Rad}}$, the fluorescence enhancement factor is of the order of $M_{\text{Fluo}} \approx M_{\text{Loc}}(\omega_L)$. Assuming $M_{\text{Loc}}(\omega_L) \approx M_{\text{Rad}}(\omega_L)$, its maximum value is of the order of $\sim 10^2 - 10^3$, and this results in a fluorescence enhancement factor of the order of $\sim 10 - 100$ after spatial averaging. This case corresponds to a "typical" situation for many MEF studies.

❖ *Non-Radiative-Emission-Dominated Substrate*

Let us now consider the same metallic NP without a dielectric spacer, i.e. the molecules adsorb directly onto the metal substrate. The non-radiative emission is then typically very large, say $M_{\text{NR}} \sim 10^5$ and dominates $\bar{M}_{\text{Tot}}$. Moreover, since it mostly depends on distance from the metal surface, it is of the same order for all molecules. All the molecules are then in the FDMEF (possibly UFDMEF) regime. $\bar{M}_{\text{Rad}}$ does not vary as much with distance from the surface and may as before have a maximum value of $\sim 10^3$. From Eq. 13, the fluorescence enhancement factor is reduced by a factor ~ 100 compared to the previous case. Overall, there is therefore no enhancement, but also *no large quenching*, as is often wrongly assumed for molecules directly adsorbed on the surface. The quenching effect of a large $\bar{M}_{\text{Tot}}$ is simply compensated by the local field enhancement factor M_{Loc} in Eq. 13. The resulting signal is still well within observation capabilities. We conclude that although the FDMEF signal intensity is typically much less enhanced (and possibly even slightly quenched) than its SDMEF counterpart, it should remain easily observable with standard techniques.

Finally, intermediate cases may obviously exist, for example at intermediate dielectric spacers or for substrates with localized regions of large radiative enhancement factors (EM hot-spots).

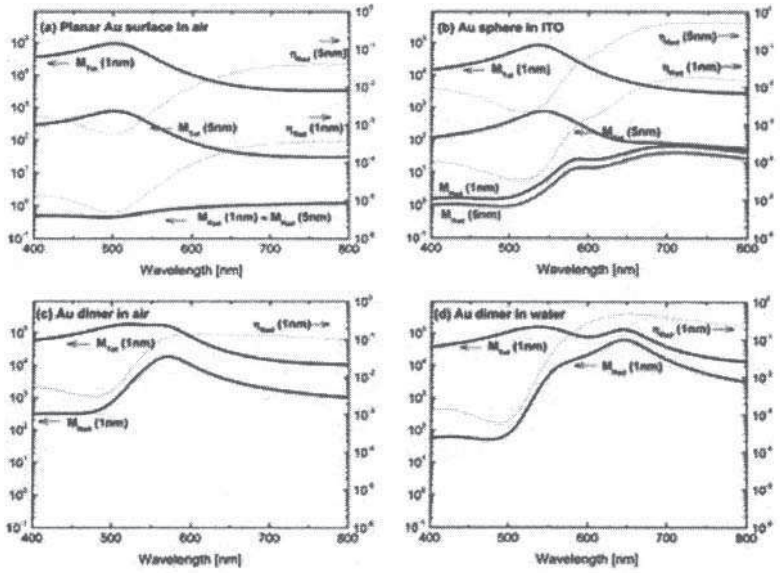

Figure 2.3: Adapted and reproduced with permission from *J. Phys. Chem. C* 2007, *111*, 16076–16079. Copyright 2007 American Chemical Society. Predictions of the frequency dependence of M_{Tot} (blue), M_{Rad} (red) (solid lines, both scale on the left axis), and the EM radiative efficiency $\eta_{\mathrm{Rad}}^{\mathrm{EM}} = M_{\mathrm{Rad}} / M_{\mathrm{Tot}}$ (dotted lines, scale on the right axis) for a dipole perpendicular to a gold metal surface and at a distance $d = 1$ nm (dark colours) or $d = 5$ nm (light colours) from the surface. Three examples are given: (a) a semi-infinite gold plane in air; (b) a gold nano-sphere of radius $a = 40$ nm in ITO (with $\varepsilon_M = 4.0$); (c-d) a dimer of two gold nano-spheres of radius $a = 30$ nm, and separated by a gap of 2 nm in either air (c) or water (d). The dipole is placed in the middle of the gap in these latter cases (i.e. $d = 1$ nm). Vertical scales have been kept the same for all three plots to facilitate the comparison of relative orders of magnitude. It is clear in these plots that M_{Tot} can be very large at short distances ($d = 1$ nm), but this does not necessarily imply a small EM radiative efficiency (and therefore a fluorescence quenching), as is the case for the planar surface.

2.3. 7.b *Examples Of EM Predictions*

To emphasize these qualitative arguments, we show in Fig. 2.3 some EM predictions for a few examples of representative geometries. M_{Tot} and

M_{Rad} can be calculated within the classical EM theory of dipolar emission [19] and we focus here on three cases for which exact results are obtainable. These are for fluorophores close to:

- a planar metal surface, [4,12]
- a metallic sphere [27]; using Mie theory,
- or a pair of metallic spheres (dimer); using Generalized Mie Theory [28,29].

Figure 2.3 shows the results of such predictions for a few representative cases (see the caption for details). The metal is gold and its dielectric function is taken from Ref. [30]. Only the case of a dipole perpendicular to the surface, at a distance d, is shown for clarity. For an emitter very close to the metal surface (typically less than 5 nm), we conclude from these model examples the following:

- For the plane and the sphere, $M_{\mathrm{Tot}} \gg M_{\mathrm{Rad}}$, i.e. the lifetime is dominated by non-radiative emission, and the EM radiative efficiency (approximate modified quantum yield) is small. We also note that M_{Tot} is then mostly determined by the distance between the metal surface and the emitter, independently of the actual geometry –and therefore of the Localized Surface Plasmon (LSP) resonances– of the metallic object. Its frequency dependence is therefore essentially governed by the intrinsic optical properties of the metal, and its magnitude depends on the distance as d^{-3} [13].

- M_{Tot} can be quite large, $\approx 10^5$ for $d = 1$ nm at the non-radiative resonance around 500 nm for gold in air (corresponding to $\varepsilon = -1$). Around 650 nm (the region of interest for the experimental results shown later in Sec. 2.4), M_{Tot} is still of the order of $\sim 10^3 - 10^4$. M_{Tot} would be even larger for a dipole closer to the surface, although a non-local dielectric function should then be used for quantitative predictions.

- For the gold dimer, M_{Rad} becomes comparable to the geometry-independent non-radiative contribution to M_{Tot}. M_{Rad} then contributes significantly to M_{Tot}. In particular, resonances of M_{Rad} are then observed in M_{Tot}, as seen in Fig. 2.3(c-d). M_{Tot} then has a relatively large radiative component, and the EM radiative efficiency or modified quantum yield can be reasonably large, $Q > 0.1$.

These predictions confirm that, in typical situations: M_{Tot} can easily be large enough for FDMEF to exist, and even possibly UFDMEF. This is

particularly true for the first few monolayers, i.e. at distances of the order of $d \approx 1$ nm or less from the surface.

2.3 7.c *Predicted intensity of the FDMEF signal*

Still, we must now consider whether in such situations any detectable fluorescence is expected. It is indeed often assumed that at such short distances the fluorescence signal would be *completely quenched* because of the dominance of non-radiative decay. This dominance is indeed a fact in many situations, and results in very poor modified quantum yields, Q, as evidenced in Fig. 2.3(a-b), but it does not necessarily imply a complete quenching of the MEF signal.

To understand this, we focus on the expression for the fluorescence EF given in Eq. 13 and recall that M_{Loc} is of the same order as M_{Rad} in a first approximation. We consider an emitter very close to the surface, say $d = 1$ nm for the sake of argument. Let us first consider the case of a planar surface (see Fig. 3(a)). M_{Rad} and M_{Loc} are of the order of 1, while $Q < 10^{-3}$, so that $M_{\mathrm{Fluo}} \approx 10^{-3} - 10^{-4}$. It is clear in this case that a large fluorescence quenching occurs, and this is partly the origin of the common view that fluorescence near metal surfaces is always quenched. Even if FDMEF exists in such a case, its intensity would not be detectable.

The situation is similar in the case of a gold sphere, because the radiative (and local field) enhancements remain small compared to M_{Tot} for $d = 1$ nm. It is interesting to note at this stage that this is not true for a silver sphere, for which the LSP resonances are much stronger (and the local field and radiative enhancements accordingly much larger); see Ref. [19] for more details. This highlights one important aspect of the optical properties of gold. Because of the large absorption for $\lambda < 600$ nm, the LSP resonances are strongly damped. At longer wavelengths however, the optical absorption of gold becomes comparable with that of silver, and much stronger LSP resonances (and therefore EFs) are then possible. To profit from these, one must have a gold structure where the LSP resonances are red-shifted to this region. This can for example be achieved by using non-spherical structures (like the ones used later), by placing the structures on a dielectric substrate (such as ITO), by making interacting structures, or by embedding the structures in a dielectric of larger dielectric constant (like water or ITO).

We have presented results in Fig. 2.3(c-d) where the resonances have been red-shifted by using interacting objects (a dimer) either in air or water. As illustrated in Fig. 2.3(c-d), it is then possible to have M_{Rad} almost comparable to M_{Tot}, and therefore a modified quantum yield of the order of $Q \sim 0.1 - 1$, even for an emitter as close as 1 nm to the surface. No quenching of the fluorescence signal is therefore predicted, and even enhancements are possible (depending on how close the dipole is to the surface) thanks to the local field enhancement effect. It should therefore be possible to observe the fluorescence signal, even in FDMEF or UFDMEF conditions.

Finally, the SERS Enhancement Factor is predicted [1] to be of the order of M_{Tot} larger than M_{Fluo}; say larger by a factor of $\sim 10^5 - 10^6$. But for typical fluorophores, the non-modified fluorescence cross-section is $\sim 10^{10}$ larger than the non-modified Raman cross-section [31]. The (integrated) MEF signal should therefore be $\sim 10^4$ times larger than the SERS signal, but it is also spread out over a much larger ($\sim 10^2 - 10^3$) spectral range than a typical SERS peak. These considerations, although mostly qualitative, show that for molecules adsorbed on the metal, the MEF signal (SDMEF or FDMEF) is expected to be at least of the order of the SERS peaks, the relative intensity depending on the exact distance of the emitter from the surface.

In conclusion, *the fluorescence signal is not necessarily completely quenched for molecules directly adsorbed on the metal surface*, but it is rather much less enhanced than the Raman signal. As a consequence, if SERS peaks can be observed for a fluorophore, they should in most cases be accompanied by a MEF signal.

2.4 EXPERIMENTAL STUDIES

The most direct approach to study the SPMs in MEF conditions is to measure the spectral profile of fluorescence under MEF conditions $I(\omega_S)$ and show that it is different to the free-space profile $n^0_{\text{Rad}}(\omega_S)$. Moreover, to confirm that the observed signal is indeed modified MEF, it is desirable to show in addition that (i) it follows the predicted profile: for example, $M_{\text{Rad}}(\omega_S)n^0_{\text{Rad}}(\omega_S)$ for SDMEF, and (ii) its intensity is compatible with the expected fluorescence enhancement.

We will present results following this approach in this section. These will be largely based on the work presented in Ref. [1]. There have not been, to our knowledge, any other dedicated experimental studies of this aspect of MEF to date in the literature. Small spectral profile modifications were however occasionally reported as part of other studies [11, 14], but have not been analyzed in depth.

2.4 1. *Experimental Considerations*

In order to carry out such a study, one must first assess carefully how the various quantities $I(\omega_S)$, $n^0_{\text{Rad}}(\omega_S)$, and $M_{\text{Rad}}(\omega_S)$ can be inferred experimentally. Let us look at each of these three aspects separately.

2.4 1.a *Free-Space Fluorescence Spectrum*

Any experimental verifications should rely on studying the modification of the fluorescence profile with respect to the free-space case. It is

therefore necessary to measure the free-space fluorescence (at the same excitation wavelength) first. Ideally, this should be carried out for the fluorophore in conditions as close as possible to the one used for MEF, i.e. in the same dielectric environment (air or water), adsorbed vs. dissolved in a solvent, etc... In any case, there is always a possibility that the intrinsic fluorescence properties of the probe are affected by adsorption onto the metallic substrate (or any dielectric spacer that may be used). For example, its electronic levels could be affected by covalent bonding to a surface or fluorophore / fluorophore interactions at large coverage. The importance of these effects should be assessed on a case-by-case basis.

In order to demonstrate large SPMs, an approximate free-space fluorescence profile is usually sufficient since the profile of the radiation enhancement factor $M_{\mathrm{Rad}}(\omega_S)$ usually dominates. For more subtle effects, like differentiating between SDMEF and FDMEF, a more accurate free-space fluorescence profile may be necessary.

2.4 1.b *Radiation enhancement and extinction profile*

Arguably the most difficult quantity to measure experimentally is the radiation enhancement factor profile $M_{\mathrm{Rad}}(\omega_S)$. It could in principle be predicted from EM theory, provided the substrate geometry is well-defined, but an experimental estimate is obviously preferred.

The simplest approach to this problem is to approximate it by the (far-field) extinction profile $Q_e(\omega_S)$, much easier to measure, i.e. $M_{\mathrm{Rad}}(\omega_S) \propto Q_e(\omega_S)$. This is justified qualitatively since both quantities are affected by coupling to the substrate localized surface plasmon resonances and should therefore exhibit the same resonances. Moreover, this approximation can be shown theoretically to be valid for simple structures like spherical nano-particles [32]. This approximation has also been used many times in the context of SERS to study the validity of the SERS EM model of the enhancement factors [21, 33, 34, 35, 36].

For a nano-particle-based substrate, additional complications may arise because of polydispersity, i.e variations in size and / or shape of the particles. This introduces changes in the LSP resonance wavelength from one particle to another and can broaden dramatically the extinction profile $Q_e(\omega_S)$. To avoid such issues, highly uniform NPs must be used. In the examples shown here, the substrates consist of arrays of gold NPs fabricated by e-beam nano-lithography [37, 38]. The high uniformity of these arrays is readily seen in the SEM images in the inset of Figs. 2.5 and 2.8 and is further confirmed by measuring the extinction $Q_e(\omega_S)$ at several positions on the array with a high magnification objective. For our purpose here, the size and shape of the particles is varied from one array to another in order to change the position of the LSP resonances, i.e. $Q_e(\omega_S)$ and therefore $M_{\mathrm{Rad}}(\omega_S)$.

2.4 1.c *MEF Spectrum And Background Subtraction*

In the experiments presented here, the fluorophores are adsorbed directly onto the metallic (gold) NP surface. The fluorescence enhancement (if any) is therefore small and the MEF signal may accordingly be weak, especially for weak fluorophores like Rh6G at 633 nm. In fact, the MEF spectrum is accompanied by Raman peaks of comparable intensity (themselves enhanced through Surface Enhanced Raman Scattering, SERS).

When considering the spectral profile of the MEF spectrum, it is extremely important to subtract any background signal not related to the NPs themselves, or at least make sure that it is negligible. The apparent profile can indeed be completely changed by the presence of a background (with its own spectral profile) of comparable intensity, as illustrated in Fig. 2.4.

Such a background may come from the environment itself (glass slide or solvent) or from fluorophores that are not adsorbed on the NPs (and therefore not under MEF conditions). In our case here, the background signal is entirely dominated by the ITO substrate supporting the gold NPs. No change in this background is detected in the presence of the fluorophores, meaning that they either do not adsorb on ITO, or that their non-enhanced fluorescence is negligible.

One can easily measure the ITO background signal $I_{\mathrm{ITO}}(\omega_S)$ by taking a spectrum under identical conditions on ITO only, for example in between two NP arrays. Subtracting directly this background from the MEF signal $I(\omega_S)$ however leads to unphysical results (negative signals in some instances). This is because, in the MEF spectrum, the ITO signal is viewed *through* the NP array and is accordingly modified because of the intrinsic extinction of the NP arrays. This can however be corrected as follows (see also Fig. 2.4).

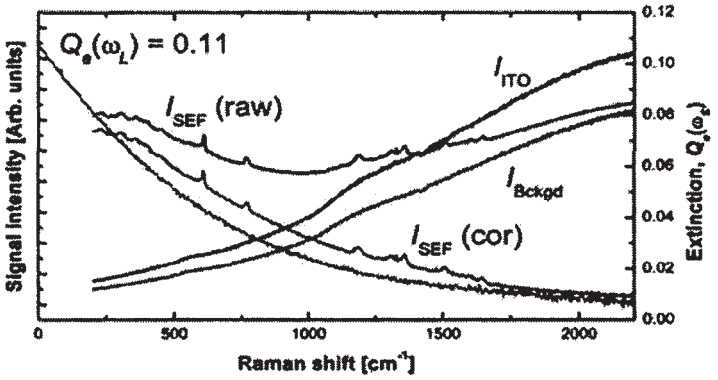

Figure 2.4: Illustration of the background subtraction for NP arrays on ITO. I_{SEF} (raw) and I_{ITO} are the raw spectra for MEF (with Rh6G adsorbed on the arrays) and ITO. Simple subtraction would result in a negative signal.

One must correct the ITO signal according to Eq. 32 to obtain the real ITO contribution, I_{Bckgd}, which once subtracted gives the corrected MEF spectrum, I_{SEF}, (cor). This step is clearly necessary here to reveal the true spectral profile of the MEF spectrum. The extinction spectrum $Q_e(\omega_S)$ for this array is also shown in the figure.

Simple subtraction would result in a negative signal. One must correct the ITO signal according to Eq. 32 to obtain the real ITO contribution, , which once subtracted gives the corrected MEF spectrum, I_{SEF} (cor). This step is clearly necessary here to reveal the true spectral profile of the MEF spectrum. The extinction spectrum $Q_e(\omega_S)$ for this array is also shown in the figure.

The extinction spectrum $Q_e(\omega_S)$ is first measured experimentally and by definition characterizes the transmission of the array at frequency ω_S:

$$Q_e = -\log_{10}\frac{I_{\text{Transmitted}}}{I_{\text{Incident}}}. \qquad (31)$$

For the MEF experiment, the incident laser at ω_L must go through the array to excite the ITO substrate. Only a fraction $10^{-Q_e(\omega_L)}$ of the power is transmitted. The ITO substrate then produces a background signal $10^{-Q_e(\omega_L)} \times I_{ITO}(\omega_S)$ (where $I_{ITO}(\omega_S)$ is the reference spectrum taken without the array), which must again go through the array before we detect it. The real ITO contribution to the MEF spectrum is therefore

$$I_{\text{Bckgd}}(\omega_S) = 10^{-Q_e(\omega_L)} \times 10^{-Q_e(\omega_S)} \times I_{ITO}(\omega_S). \qquad (32)$$

This background should be removed before any interpretation of the MEF spectrum. The effect could be dramatic in some situations as illustrated in Fig. 2.4. This is not as critical when the MEF intensity is much larger than the ITO background (which is generally the case for Methylene Blue (MB) or Crystal Violet (CV) for example).

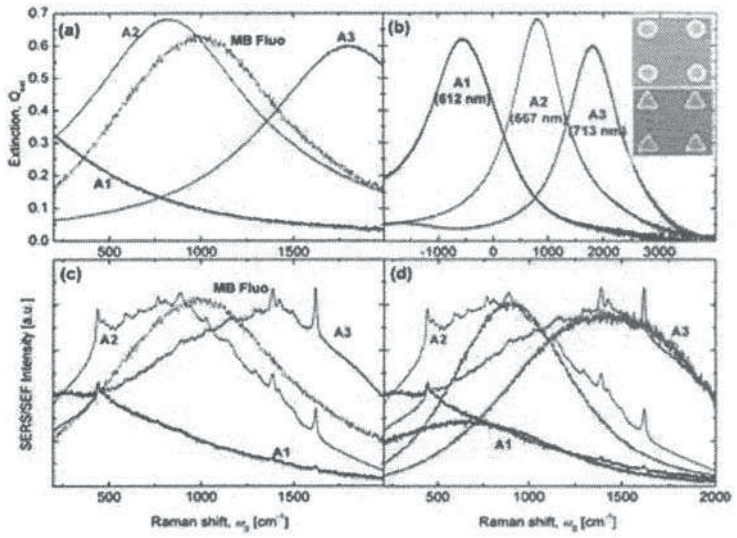

Figure 2.5: Reproduced with permission from *J. Phys. Chem. C* 2007, *111*, 16076–16079. Copyright 2007 American Chemical Society. (a-b) Extinction spectra ($Q_{\text{ext}}(\omega_S)$) for three gold nanoparticle arrays: A1 (100 nm edge triangles), A2 (100 nm diameter dots), and A3 (150 nm edge triangles). Resonance wavelengths for each are indicated in brackets in (b); representative SEM images are shown in the inset. The data in (a) are the same as in (b), but on the same energy scale as used in (c) and (d) for easier comparison. (c) SERS / SMF spectra at 633 nm excitation of the same arrays, covered with methylene blue (MB). The standard MB fluorescence (adsorbed on ITO), $P^0_{\text{Fluo}}(\omega_S)$, is shown in (a) and (c). (d) Comparison of the SMF spectra of (c) with the approximated predicted profile: $Q_{\text{ext}}(\omega_S)P^0_{\text{Fluo}}(\omega_S)$.

2.4 2. *Evidence Of Spectral Profile Modifications*

One possible approach to evidence strong spectral profile modifications under MEF conditions is to take a given fluorophore (fixed $n^0_{\text{Rad}}(\omega_S)$), and vary the radiation enhancement factor profile $M_{\text{Rad}}(\omega_S)$. The MEF spectral profile should then change in the same direction as $M_{\text{Rad}}(\omega_S)$. The change in $M_{\text{Rad}}(\omega_S)$ can, for example, be obtained by changing the size and / or shape of the gold NPs and is easily monitored by measuring their extinction spectrum $Q_e(\omega_S)$.

An example of the results for such an approach is shown in Fig. 2.5 (from Ref. [1]), which we now discuss. Methylene Blue (MB) is used here as a probe molecule and is transferred onto gold NP arrays by dipping them into a 10 μM MB solution for 5 minutes. The arrays are plasma-cleaned before any dipping, to ensure that no contaminants are previously adsorbed on the NPs. The MB molecules are therefore adsorbed directly onto the gold surfaces, with possibly some molecules further away from the surface if several monolayers are present. Three NP arrays are used with distinct LSP resonances at 612 nm (array A1), 667 nm (A2) and 713 nm (A3), as evidenced in the extinction spectra of Fig. 2.5(b). The resonance of A2 is close to the peak absorption and fluorescence of MB and would be considered as the "standard" situation for most MEF experiments (except for the direct adsorption onto the metal). A1 and A3 have resonances much further away on either side of the MB fluorescence spectrum. The MEF spectra (corrected for the ITO background), shown in Fig. 2.5(c), exhibit a broad spectrum underneath the SERS (Raman) peaks. The SERS peaks clearly confirm the presence of MB on the NPs surface. The accompanying broad signal is attributed to the modified MB fluorescence (MEF), initially for two reasons:

- The signal is not observed in the absence of adsorbed molecules (MB or otherwise). Note that a thorough cleaning (plasma cleaning in this case) is necessary to ensure that no spurious fluorescent species remain on the sample.

- The broad signal (and the SERS peaks) decays as a result of photobleaching, and the signal decay rates increase with excitation density.

This interpretation is further confirmed by comparison with the predicted modified MEF spectral profile. For this, we make the assumption discussed earlier that $M_{\mathrm{Rad}}(\omega_S) \propto Q_e(\omega_S)$, and $n^0_{\mathrm{Rad}}(\omega_S)$ can be approximated by the free-space fluorescence profile $P^0_{\mathrm{fluo}}(\omega_S)$ of MB dried on ITO (at high concentration). Hence, the MEF profile (for SDMEF) should follow the product $Q_e(\omega_S)P^0_{\mathrm{fluo}}(\omega_S)$, which is indeed the case to a good approximation as shown in Fig. 2.5(d). The results of Fig. 2.5 demonstrate clearly the possibility of a large spectral profile modification under MEF conditions.

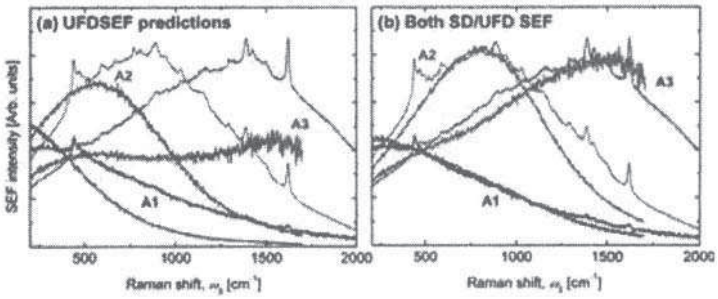

Figure 2.6: (a) Comparison of the experimental results of Fig. 5 for MB on arrays A1, A2, and A3 with theoretical predictions in the UFDMEF regime with $\Delta\omega_L = 700$ cm^{-1}, i.e. $Q_e(\omega_S)n^0_{\text{Rad}}(\omega_S - \Delta\omega_L)$. (b) Same as (a) using a weighted superposition of the theoretical predictions in the SDMEF regime (shown in Fig. 2.5(d)) and in the UFDMEF regime (shown in (a)).

2.4 3. *Evidence For Fast-Dynamics MEF*

The comparison between experiments and SDMEF predictions in Fig. 2.5(d) also validates the simple model presented earlier. One may notice however, that the SDMEF predictions tend to underestimate the short-wavelength side of the modified MEF spectra. This could be a consequence of some molecules being in the FDMEF (or UFDMEF) regimes. It would qualitatively enhance more the short-wavelength side of the spectrum at the expense of the other side as predicted theoretically in Fig. 2.2(d).

To be more quantitative, it is possible to compare the experimental MEF results to the UFDMEF predictions, i.e. to the product $Q_e(\omega_S)P^0_{\text{fluo}}(\omega_S - \Delta\omega_L)$. This is illustrated in Fig. 2.6(a). It is clear that the UFDMEF spectra can explain the discrepancies observed in the SDMEF spectra, but then the long-wavelength side of the spectrum is no longer correctly predicted. Only a weighted superposition of both the SDMEF and UFDMEF predictions results in a better account of the overall spectral profile under MEF conditions, as shown in Fig. 2.6(b). This result can be interpreted in two ways: (i) The majority of molecules are in the intermediate FDMEF regime, where internal relaxation rates are comparable to decay rates. As discussed in Sec. 2.3, an intermediate spectrum between the SDMEF and UFDMEF cases is then expected. Unfortunately, the details of such a spectrum are difficult to predict theoretically. (ii) The total decay rate enhancement factors are non-uniform on the surface, resulting in some molecules being in SDMEF conditions, while other are in FDMEF or even UFDMEF conditions. This could for example be the case if some molecules are further away from the surface (i.e. for multilayer coverage). It is difficult from the sole evaluation of the optical spectra to distinguish between these two scenarios.

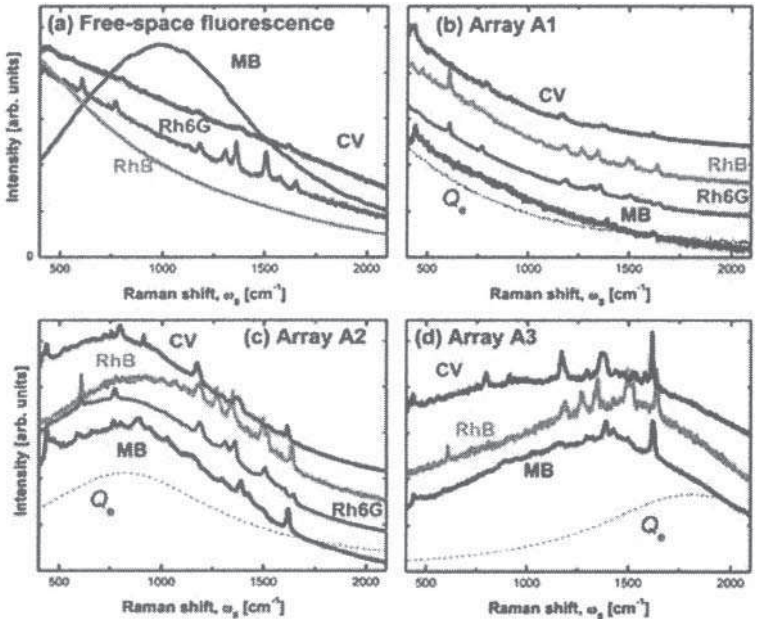

Figure 2.7: (a) Free-space fluorescence spectra ($P^0_{\text{Fluo}}(\omega_S)$) for four fluorophores: Methylene Blue (MB), Rhodamine 6G (Rh6G), Rhodamine B (RhB), and Crystal Violet (CV). (b-d) MEF spectra obtained from arrays A1 (b), A2 (c), and A3 (d) after dipping in a 10 μM solution for each of the four fluorophores in (a). All spectra are obtained for excitation at 633 nm and are shown in terms of the Raman shift (equivalent to ω_S). All spectra intensities have been rescaled and are displaced vertically in (b-d) for convenience. The extinction profile $Q_{\text{ext}}(\omega_S)$ for each array is also shown in (b-d) as a dashed line. Note that the spectrum for Rh6G on array A3 was not measured.

2.4 4. *Comparison Between Different Fluorophores*

Another complementary approach to that presented so far is to study different fluorophores (with different free-space fluorescence spectral profiles) on the same NP arrays. This is illustrated in Fig. 2.7. Four fluorophores are used there: Methylene Blue (MB) as before, Rhodamine 6G (Rh6G), Rhodamine B (RhB), and Crystal Violet (CV). All experiments are carried out at 633 nm excitation again, and the corresponding free-space fluorescence spectra are shown in Fig. 2.7(a). Rh6G, RhB, and CV all exhibit a tail-like fluorescence spectrum, very similar to each other. This simply reflects the fact that the excitation (at 633 nm) is close or below (in energy) the main absorption band. In this case, internal relaxation in S_1 is expected to play a negligible role, even

in free-space conditions. The SDMEF and FDMEF regimes should therefore be equivalent for these three molecules. It should also be similar to the UFDMEF spectrum of any molecules as discussed in Sec. 2.3 5. In fact, similar MEF spectral profiles are obtained for the four molecules on each of the three NP arrays as shown in Fig. 2.7(b-d). The fact that the results for MB are similar to the other three molecules –despite their dissimilar free-space fluorescence spectra– is further indication that the MB molecules are in the FDMEF regimes (possibly UFDMEF for some).

The spectra in Fig. 2.7 also further confirm the possibility of large spectral profile modifications in MEF conditions.

2.4 5. *Discussion Of The Experimental Results*

The SPMs observed in Figs 2.5, 2.6, 2.7 are sufficiently large and unambiguous to render a clear-cut identification of spectral modifications of the emission. The agreement between experimental and predicted spectra is also sufficiently satisfactory to support the interpretations and validate the models (despite their simplicity). Nonetheless, a more accurate agreement would be desirable for subtler effects, such as a clear distinction between SDMEF and (U)FDMEF. This is, however, prevented by a number of issues; which we highlight here as a prerequisite towards improved future experiments.

❖ As already mentioned, the "free-space" fluorescence profile may be modified upon molecular adsorption, even before any modifications associated with the EM response of the substrate. This may arise from small alterations in their electronic structure or from molecule / molecule interactions (at high coverage). Unfortunately, there is no simple experimental solution to this issue. One approach is to use several different fluorophores; any strong modifications for one of them will result in anomalous behaviour with respect to the others.

❖ The approximation of the radiation enhancement factor profile $M_{\mathrm{Rad}}(\omega_S)$ by the extinction spectrum $Q_e(\omega_S)$ may not always be valid. EM calculations on the NPs may be used to confirm it.

❖ In all the results shown here, the extinction spectra were measured on bare substrates (not covered with molecules). However, it has been shown that molecular adsorption may affect the underlying LSP resonances and therefore change slightly the extinction profiles [39]. This aspect can be improved upon by measuring the extinction spectrum of the arrays for each molecule.

❖ The theoretical description of the fluorescence process, even for free-space fluorescence, could be improved. For example, the relevance (if any) of the internal relaxation in S_1 for excitation in the fluorescence tail below the adsorption band is not well understood. Moreover, the description of the intermediate FDMEF regime requires a detailed understanding of the internal

relaxation mechanisms in S_1. Further improvements to account for temperature-related effects in the effective populations of S_0 and S_1 can also be envisioned.

These secondary aspects do not affect the main conclusions of this section, but would certainly contribute to a deeper understanding of the SPMs mechanisms in MEF.

2.5 ADVANCED ASPECTS AND OUTLOOK

2.5 1. *The SERS Continuum*

An interesting aspect of the large spectral profile modifications that may arise in MEF conditions is the fact that the resulting spectrum is modified to an extent that it may not be easily recognized as a fluorescence spectrum. This means that it may be observed in many standard experimental situations but incorrectly interpreted. Along these lines, we propose that this modified MEF (either SDMEF with a large SPM or FDMEF) may be the origin of the so-called SERS continuum in many common situations (and in particular for dyes, even weakly fluorescent). Such an interpretation is compatible with many well-known features of the SERS continuum [14, 40, 41, 42, 43, 44] which, following Ref. [1], are listed below along with other important predictions of this proposal:

- The SDMEF / FDMEF follows the same intensity fluctuations and polarization properties of the SERS signal through the factor $M_{\mathrm{Rad}}(\omega_S)$, as observed for the SERS continuum.

- There is no MEF in the absence of adsorbed molecules, as for the SERS continuum. We note that this is still a contentious point in relation to the SERS continuum itself, since there are conflicting reports of whether the SERS continuum is observed or not in the absence of adsorbed molecules. These have been tentatively attributed to problems of surface cleanliness and impurities [41]. Our experiments support this view: the MEF / SERS background only disappears upon thorough plasma cleaning.

- The issue of surface cleanliness and impurities is even more problematic for non-resonant molecules, since the SERS signals are much smaller [31] and therefore potentially more affected by contaminations. The MEF from organic impurities [41] could therefore account for the SERS background of non-resonant molecules.

- Contrary to what is generally thought, MEF is possible even for molecules in direct contact with the metal, as is often the case in SERS. This was shown and discussed extensively in Sec. 2.3 7.

❖ The underlying resonance that should characterize the SPM of the MEF (and therefore the SERS background within our proposal) is not seen in most SERS experiments because of its large inhomogeneous broadening for most substrates and the typically small spectral window usually probed with high dispersion gratings. Our ability to identify it as such in Figs. 2.5, 2.6, 2.7 is a direct consequence of the high uniformity of the resonances in our structures and the wide spectral window.

❖ As mentioned, in UFDMEF conditions, the spectral profile is mostly independent of the molecule, and could therefore account for the lower energy peak of the SERS continuum observed in Ref. [14] (previously attributed to electronic Raman scattering or to LSP luminescence).

❖ One interesting consequence of the MEF interpretation concerns the behaviour of the SERS background when changing laser excitation. Depending on the specific SERS conditions, the background may consist of either SDMEF, FDMEF (possibly UFDMEF), or both. When changing excitation wavelength, the SDMEF signals should retain their spectral profile, but the FDMEF should be shifted together with the laser in a similar fashion as a Raman signal, thus potentially explaining conflicting reports regarding the actual nature (Raman vs. luminescence) of the SERS background.

This proposal obviously requires further investigation. It is clear, however, that the possibility of a MEF background (possibly strongly modified spectrally) should be considered in any interpretations of the SERS continuum. It is likely that this could account for many (if not all) observations of the SERS continuum, in particular for SERS of resonant or pre-resonant analytes such as dyes. In fact, in all the spectra presented in this chapter, the SERS signal is clearly observed and the underlying background could have been ascribed from a SERS perspective to a "SERS continuum" of unknown origin.

2.5 2. *Polarization Effects*

In the theoretical and experimental discussion presented so far, we have not discussed any polarization effects such as: (i) the dependence of the LSP resonances upon the incident polarization, or (ii) the nature of the polarization of the emitted fluorescence signal. This choice simplified the presentation of the principles of SPM in MEF and did not affect the interpretations of the experimental results, which were obtained from NP arrays with no (or only a weak) polarization dependence.

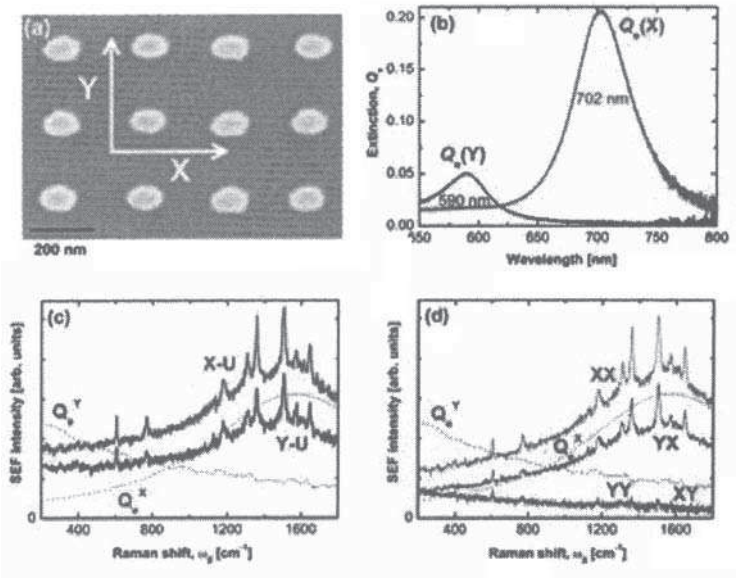

Figure 2.8: Adapted and reproduced with permission from *J. Phys. Chem. C* 2008, *112*, 8117-8121. Copyright 2008 American Chemical Society. (a) Representative SEM image of gold prolate NPs. Height is ≈ 50 nm and dimensions in the plane are 140 nm (X) by 90 nm (Y) (b) Extinction spectrum, Q_e^X and Q_e^Y, for X - and Y -polarized excitation. (c) MEF spectra at 633 nm excitation after dipping the array in a 10^{-5} M Rh6G solution. SERS peaks can be seen on top of the modified MEF spectrum. Detection is unpolarized and excitation is polarized along X ($X-U$) or Y ($Y-U$). Also shown (dashed lines) are the extinction spectra Q_e^X and Q_e^Y, for X - and Y -polarized excitation. The spectral profile of MEF follows $Q_e^X(\omega_S)$ in both cases. (d) MEF spectra for E -polarized excitation and D -polarized detection (i.e. four configurations, $ED = XX$, XY, YX, YY). It is clear that the MEF spectral profile follows Q_e^D, i.e. it is *determined by the detection polarization.* The excitation polarization only affects the overall MEF intensity. As a consequence, the MEF signal for Y -polarized excitation is almost entirely X -polarized (YX is much larger than YY).

It is however possible to design specifically NP arrays with a strong polarization dependence in order to investigate polarization effects. This has recently been reported [21] using arrays of "elongated" gold NPs (with elliptic cross-section), which exhibit two distinct LSP resonances, each associated with a polarization along the two main axis of the ellipse. The spectral response for

each resonance, $Q_e^X(\omega)$ and $Q_e^Y(\omega)$, can be measured by polarized extinction measurements. Some of the results of this study are illustrated in Fig. 2.8, which is explained in the caption. We mention here briefly the main conclusions:

- The incident polarization only affects the coupling to the LSP resonances at the laser frequency ω_L, i.e. the local field enhancement factor at ω_L. It has no effect on the spectral profile of fluorescence.

- The MEF spectrum is in general affected by both resonance profiles $Q_e^X(\omega_S)$ and $Q_e^Y(\omega_S)$.

- The respective contributions of these two resonances can be separated experimentally by analyzing the polarization of the MEF signal. The MEF signal for polarized detection along X simply follows a spectral profile $\approx Q_e^X(\omega_S) n_{\text{Rad}}^0(\omega_S)$ (and similarly for Y).

- A rather spectacular consequence of this is that the spectral profile of MEF for a given fluorophore adsorbed on a given array may be dramatically different when analyzed with one polarization or the other. Along the same line, the fluorescence depolarization ratio is predominantly dictated by the underlying LSP resonances and is therefore ω_S-dependent and can, under appropriate conditions, be as large as ≈ 10, i.e. there is an almost complete *polarization rotation* of the MEF spectrum with respect to the incident polarization.

These experimental results confirm and extend the interpretations given earlier. We refer the reader to Ref. [21] for further details and discussion of these results in the context of SERS and in relation to surface selection rules [45, 46].

2.5 3. *Further Experiments*

The experimental results presented so far demonstrate clearly the existence of a strong SPM in MEF conditions. However, it remains difficult to distinguish between the Slow-Dynamics and Fast-Dynamics regime of MEF from these results. Additional experiments can be envisaged to provide more direct evidence for FDMEF and study the transition between these two regimes. The easiest approach (possibly) would be to carry out a distance-dependence study of the MEF; for example using dielectric spacers. If non-radiative emission is important for molecules directly adsorbed on the metal, its proportion should decrease dramatically as the molecule moves away from the surface (even by a few nm), i.e. the decay rate Γ_{Tot} becomes slower and SDMEF becomes more likely. In the meantime, the spectral profile of the radiative enhancement factor $M_{\text{Rad}}(\omega_S)$ is not expected to vary much. Any

spectral profile changes as a function of distance would therefore be a strong indication of a transition from a FDMEF- (or UFDMEF-) dominated regime to a SDMEF regime.

Another interesting extension of the experiments presented here would be to study the SPM of the MEF in *single molecule* (SM) conditions. The SERS signal of single fluorescing molecules are now routinely observed [47, 48], and one would then only need to study the accompanying fluorescence background. Unfortunately, single molecule SERS has not been yet achieved *in highly controlled conditions* and many problems may therefore arise in the interpretation of the results. It is in particular difficult to (i) measure the underlying LSP resonance associated with a given SM event, and (ii) measure and subtract the background signal not associated with the SM event (extrinsic fluorescence, etc...).

2.5 4. *Conclusion And Outlook*

With the benefit of hindsight, it is possible to claim that spectral modifications of the fluorescence profile have been to a large degree overlooked in the literature, although occasionally hinted at [11, 22, 23]. But this oversight can be easily understood in many ways. For a start, most studies in the past have focused on the seemingly more "urgent" matter of total (spectrally integrated) properties of fluorophores on surfaces; and in particular on the very important question of whether the dyes will emit *more* or *less* overall fluorescence through the interaction. The effects described here, however, are a step forward in our basic understanding of fluorescence emission in close proximity of surfaces. By including explicitly in the treatment the *spectral modification* of the emission, a new dimension is added to the problem and new directions are immediately evident. From a wider standpoint, it is to some extent paradoxical that one of the clearest effects revealed by the spectral modification of the fluorescence arises from optical excitation in the low energy *tail* of the absorption of a dye (as in the case of Rh6G at 633 nm). This situation produces a fairly featureless background fluorescence emission that is more susceptible then to reveal the spectral profile of the underlying plasmon resonances. Indeed, it is worth noting that this is a situation that would be deemed as *not very interesting* in the realms of conventional fluorescence spectroscopy (where one would try to excite as much fluorescence as possible by using an excitation at much shorter wavelengths tuned to the dye absorption). This latter point is, in fact, partially (but not completely) responsible for the delay hitherto in the published literature to single out the phenomenon of *spectral modification of the fluorescence emission* as an "effect in its own right".

Undoubtedly –together with an improved understanding of the fluorescence process itself– many possible new paths are now open for further research and the results highlighted in this chapter have much wider implications. The striking connection with the "elusive" nature of SERS backgrounds mentioned in Sec. 2.5, for example, is certainly one such promising area of likely future developments. As it stands at the moment, we would argue the spectral profile modification of the MEF signal provides the most natural explanation to all the known phenomenology of SERS backgrounds. If this

latter connection is confirmed by future research, a new layer of understanding will emerge in the related technique of SERS. This would also tighten the link between the two techniques, SERS and MEF, which despite their common "plamonics" basis, have been largely studied so far as two independent entities.

2.6 NOTE

A number of recent papers dealing with similar concepts as those discussed in this chapter have appeared in the literature [49,50,51] after the writing of this manuscript.

Some of the basic electromagnetic models mentioned here are also extensively discussed in Ref. [52].

2.7 ACKNOWLEDGMENT

This work was supported by the Dumont d'Urville France/NZ exchange programme.

2.7 REFERENCES

1 Le Ru, E. C., Etchegoin, P. G., Grand, J., Félidj, N., Aubard, J., and Lévi, G. (2007). Mechanisms of Spectral Profile Modification in Surface-Enhanced Fluorescence. *J. Phys. Chem. C* **111**:16076–16079; see also Supplementary info.

2 Philpott, M. R. (1975). Effect of surface plasmons on transitions in molecules. *J. Chem. Phys.* **62**:1812–1817.

3 Morawitz, H., and Philpott, M. R. (1974). Coupling of an excited molecule to surface plasmons. *Phys. Rev. B* **10**:4863–4868.

4 Chance, R. R., Prock, A., and Silbey, R. (1978). Molecular fluorescence and energy transfer near interfaces. *Adv. Chem. Phys.* **37**:1–65.

5 Metiu, H. (1984). Surface enhanced spectroscopy. *Progress. Surf. Sci.* **17**:153–320; and references therein.

6 Ford, G. W., and Weber, W. H. (1984). Electromagnetic interactions of molecules with metal surfaces. *Phys. Rep.* **113**:195–287; and references therein.

7 Dulkeith, E., Morteani, A. C., Niedereichholz, T., Klar, T. A., Feldmann, J., Levi, S. A., van Veggel, F. C. J. M., Reinhoudt, D. N., Möller, M., and Gittins, D. I. (2002). Fluorescence quenching of dye molecules near gold nanoparticles: Radiative and nonradiative effects. *Phys. Rev. Lett.* **89**:203002-1–4.

8 Geddes, C. D., and Lakowicz, J. R. (2002). Metal-enhanced fluorescence. *J. Fluoresc.* **12**:121–129.

9 Lakowicz J. R., Geddes, C. D., Gryczynski, I., Malicka, J., Gryczynski, Z., Aslan, K., Lukomska, J., Matveeva, E., Zhang, J., Badugu, R., and Huang, J. (2004). Advances in surface-enhanced fluorescence. *J. Fluoresc.* **14**:425–441.

10 Anger, P., Bharadwaj, P., Novotny, L. (2006). Enhancement and Quenching of Single-Molecule Fluorescence. *Phys. Rev. Lett.* **96**:113002-1–4.

11 Kühn, S., Hakanson, U., Rogobete, L., and Sandoghdar, V. (2006). Enhancement of ingle-Molecule Fluorescence Using a Gold Nanoparticle as an Optical Nanoantenna. *Phys. Rev. Lett.* **97**:017402-1–4; see also Supplementary info.

12 Novotny, L., and Hecht, B. (2006). *Principles of Nano-Optics*. Cambridge University Press, Cambridge.

13 Bharadwaj, P., and Novotny, L. (2007). Spectral dependence of single molecule fluorescence enhancement. *Optics Express* **15**:14266–14274.

14 Maruyama, Y., and Futamata, M. (2005). Elastic scattering and emission correlated with single-molecule SERS. *J. Raman Spectrosc.* **36**:581–592.

15 Valeur, B. (2002). *Molecular Fluorescence. Principles and Applications*. Wiley-VCH, Weinheim.

16 Lakowicz, J. R. (2006). *Principles of Fluorescence Spectroscopy*, 3rd ed. Springer, New York.

17 Das, P., and Metiu, H. (1985). Enhancement of molecular fluorescenceand photochemistry by small metal particles. *J. Phys. Chem.* **89**:4680–4687.

18 Barnett S. M., Huttner B., and Loudon R. (1992). Spontaneous emission in absorbing dielectric media. *Phys. Rev. Lett.* **68**:3698–3701.

19 Le Ru, E. C., and Etchegoin, P. G. (2005). Surface-Enhanced Raman Scattering (SERS) and Surface-Enhanced Fluorescence (SEF) in the context of modified spontaneous emission. arXiv:physics/0509154v1 pp.1–14.

20 Le Ru, E. C., and Etchegoin, P. G. (2006). Rigorous justification of the $|E|^4$ enhancement factor in Surface Enhanced Raman Spectroscopy *Chem. Phys. Lett.* **423**:63–66.

21 Le Ru, E. C., Grand, J., Félidj, N., Aubard, J., Lévi, G., Hohenau, A., Krenn, J. R., Blackie E., Etchegoin, P. G. (2008). Experimental verification of the SERS electromagnetic model beyond the $|E|^4$-approximation: polarization effects. *J. Phys. Chem. C* in press.

22 Ritchie, G., and Burstein, E. (1981). Luminescence of dye molecules adsorbed at a Ag surface. *Phys. Rev. B* **24**:4843–4846.

23 Leitner, A., Lippitsch, M. E., and Aussenegg, F. R. (1983). in *Surface Studies with Lasers"*. Springer, Berlin.

24 Atherton, S. J., and Harriman, A. (1993). Photochemistry of intercalated methylene blue: photoinduced hydrogen atom abstraction from guanine and adenine. *J. Am. Chem. Soc.* **115**:1816–1822.

25 Eggeling, C., Widengren, J., Rigler, R., and M. Seidel, C. A. (1998). Photobleaching of fluorescent dyes under conditions used for single-molecule detection: evidence of two-step photolysis. *Anal. Chem.* **70**:2651–2659.

26 Le Ru, E. C., Etchegoin, P. G., and Meyer, M. (2006). Enhancement factor distribution around a single SERS hot-spot and its relation to single molecule detection. *J. Chem. Phys.* **125**:204701-1–13.

27 Chew, H. (1987). Transition rates of atoms near spherical surfaces. *J. Chem. Phys.* **87**:1355–1360.

28 Gérardy, J. M., and Ausloos, M. (1982). Absorption spectrum of clusters of spheres from the general solution of Maxwell's equations. II. Optical properties of aggregated metal spheres. *Phys. Rev. B* **25**:4204–4229.

29 Johansson, P., Xu, H., and Käll, M. (2005). Surface-enhanced Raman scattering and fluorescence near metal nanoparticles. *Phys. Rev. B* **72**:035427-1–17.

30 Etchegoin, P. G., Le Ru, E. C., and Meyer, M. (2006). An analytic model for the optical properties of gold. *J. Chem. Phys.*, **125**:164705-1–3.

31 Le Ru, E. C., Blackie, E., Meyer, M., and Etchegoin, P. G. (2007). Surface Enhanced Raman Scattering Enhancement Factors: A Comprehensive Study. *J. Phys. Chem. C* **111**:13794–13803.

32 Messinger, B. J., von Raben, K. U., Chang, R. K., and Barber, P. W. (1981). Local fields at the surface of noble-metal microspheres. *Phys. Rev. B* **24**:649–657.

33 Félidj, N., Aubard, J., Lévi, G., Krenn, J. R., Salerno, M., Schider, G., Lamprecht, B., Leitner, A., and Aussenegg, F. R. (2002). Controlling the optical response of regular arrays of gold particles for surface-enhanced Raman scattering. *Phys. Rev. B* **65**:075419-1–9.

34 Haynes, C. L., and Van Duyne, R. P. (2003). Plasmon-Sampled Surface-Enhanced Raman Excitation Spectroscopy. *J. Phys. Chem. B*, **107**:7426–7433.

35 McFarland, A. D., Young, M. A., Dieringer, J. A., and Van Duyne, R. P. (2005). Wavelength-Scanned Surface-Enhanced Raman Excitation Spectroscopy. *J. Phys. Chem. B* **109**:11279–11285.

36 Le Ru, E. C., Etchegoin, P. G., Grand, J., Félidj, N., Aubard, J., Lévi, G., Hohenau, A., Krenn, J. R. (2008). Surface Enhanced Raman Spectroscopy on Nano-lithography-prepared substrates. *Cur. Appl. Phys.* **8**:467–470.

37 McCord, M. A., and Rooks, M. J. (1997). Electron Beam Lithography. In *Handbook of Microlithography, Micro matching and Micro fabrication. Volume 1: Microlithography*, P. Rai-Choudhury (Ed.), SPIE press book, Washington, pp. 139–250.

38 Gold arrays are prepared by electron beam lithography (EBL) according to the following method. The bare substrate is a glass plate (10 mm × 10 mm) on which a thin indium tin oxide (ITO) substrate is evaporated. The ITO substrate is then spin coated (60 s, at 5000 rpm) with a 100 nm thick Poly methyl-methacrylate (PMMA) polymer, baked at 170 ° C for 8 hours and exposed in an electron-beam writing

equipment consisting of a JEOL 6400 scanning electron microscope (SEM) and a RAITH Quantum pattern generator. After exposure, a chemical development is performed by a 1:2 mixture of developer (PMMA-developer, Allresist Comp.) and isopropanol. The resulting PMMA film is then used as a mask for the thermally deposition of a 40 nm thick gold layer. Removing the remaining PMMA layer by a chemical lift off process leaves gold particles on the ITO substrate at the position defined by the e-beam exposure. The array size is a square of 100 μ m side length.

39 Zhao, J., Jensen, L., Sung, J., Zou, S., Schatz, G. C., and Van Duyne, R. P. (2007). Interaction of Plasmon and Molecular Resonances for Rhodamine 6G Adsorbed on Silver Nanoparticles. *J. Am. Chem. Soc.* **129**:7647–7656.

40 Jiang, J., Bosnick, K., Maillard, M., Brus, L. (2003). Single Molecule Raman Spectroscopy at the Junctions of Large Ag Nanocrystals. *J. Phys. Chem. B* **107**:9964–9972.

41 Maruyama, Y., Futamata M. (2005). Inelastic scattering and emission correlated with enormous SERS of dye adsorbed on Ag nanoparticles. *Chem. Phys. Lett.* **412**:65–70.

42 Moskovits, M. (2005). Surface-enhanced Raman spectroscopy: a brief retrospective. *J. Raman Spectrosc.* **36**:485–496.

43 Itoh, T., Biju, V., Ishikawa, M., Kikkawa, Y., Hashimoto, K., Ikehata, A., Ozaki, Y. (2006). Surface-enhanced resonance Raman scattering and background light emission coupled with plasmon of single Ag nanoaggregates. *J. Chem. Phys.* **124**:134708-1–6.

44 Itoh, T., Kikkawa, Y., Biju, V., Ishikawa, M., Ikehata, A., Ozaki, Y. (2006). Variations in Steady-State and Time-Resolved Background Luminescence from Surface-Enhanced Resonance Raman Scattering-Active Single Ag Nanoaggregates. *J.Phys. Chem. B* **110**:21536–21544.

45 Moskovits, M. (1982). Surface Selection Rules. *J. Chem. Phys.* **77**:4408–4416.

46 Le Ru, E. C., Meyer, M., Blackie, E., and Etchegoin, P. G. (2008). Advanced aspects of electromagnetic SERS enhancement factors at a hot spot. *J. Raman Spectrosc.* in press.

47 Le Ru, E. C., Meyer, M., and Etchegoin, P. G. (2006). Proof of Single-Molecule Sensitivity in Surface Enhanced Raman Scattering (SERS) by Means of a Two-Analyte Technique. *J. Phys. Chem. B* **110**:1944–1948.

48 Pieczonka, N. P. W., Aroca, R. F. (2008). Single molecule analysis by surfaced-enhanced Raman scattering. *Chem. Soc. Rev.*, in press, doi:10.1039/b709739p.

This Page Intentionally Left Blank